HST Observations of Escaping LyC Radiation from Galaxies & weak AGN at $2.3 \lesssim z \lesssim 5$: (How) Did they Reionize the Universe, and what JWST must do next.

Rogier Windhorst (ASU) — JWST Interdisciplinary Scientist

Brent Smith, S. Cohen, R. Jansen, L. Jiang, M. Dijkstra, A. Inoue,

A. Koekemoer, R. Bielby, J. MacKenty, R. O'Connell, & J. Silk

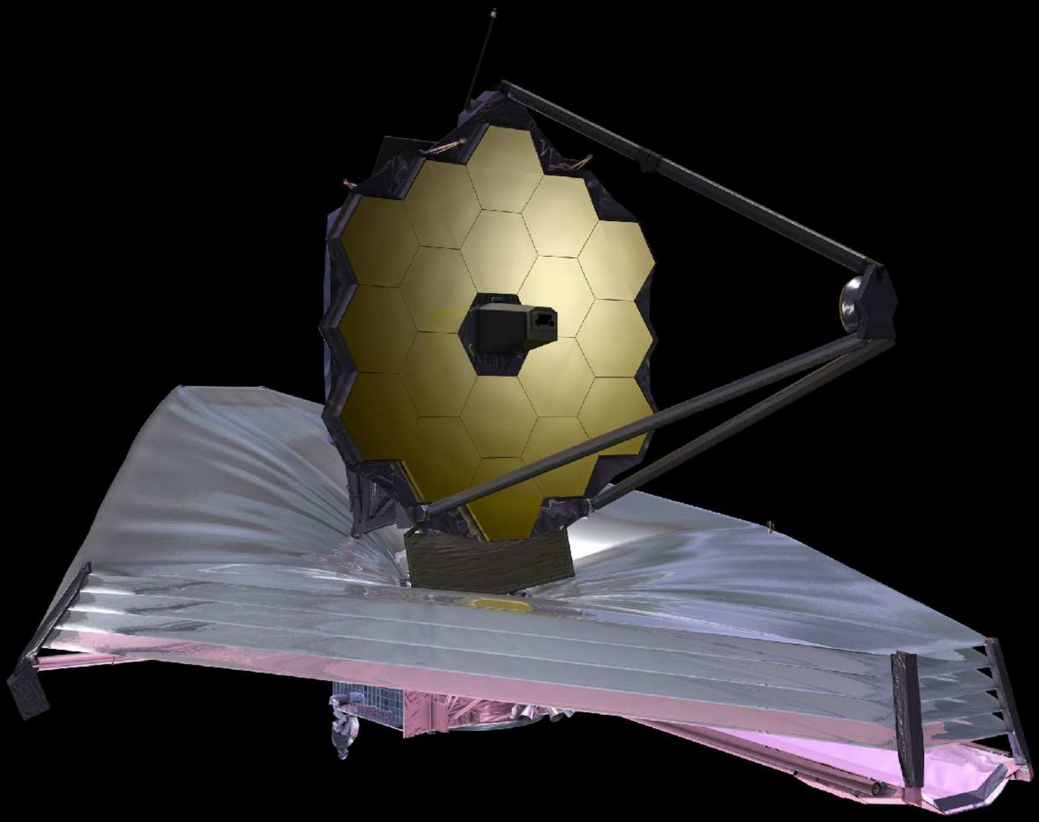

Talk at the Lagrange Institute Conference on "Cosmology and First Light"

Monday December 7, 2015; Institute d'Astrophysique, Paris, France

Outline

- (1) HST WFC3 Data & Spectroscopic Sample Selection
- (2) WFC3 & ACS Lyman Continuum Stacking, Systematics, & Fluxes
- (3) Stacked Lyman-Continuum and UV-Continuum Light-Profiles
- (4) SED-fitting & Dust-distribution $A_V(z)$
- (5) LyC Escape Fractions vs. z for Faint Galaxies & Weak AGN
- (6) What critical aspects will JWST add to LyC Escape studies?
- (7) Summary and Conclusions

Sponsored by NASA/HST & JWST

ASU Arizona State University

Talk is on: http://www.asu.edu/clas/hst/www/jwst/jwsttalks/paris15_jwstlyc.pdf

In what follows, remember that objects emitting two-sided and equally bright relativistic jets, or escaping LyC radiation may look *different*, depending, e.g. on viewing angle, dust, and scattering properties of the medium.

(1a) Hubble WFC3 Data: The Early Release Science (ERS) field.

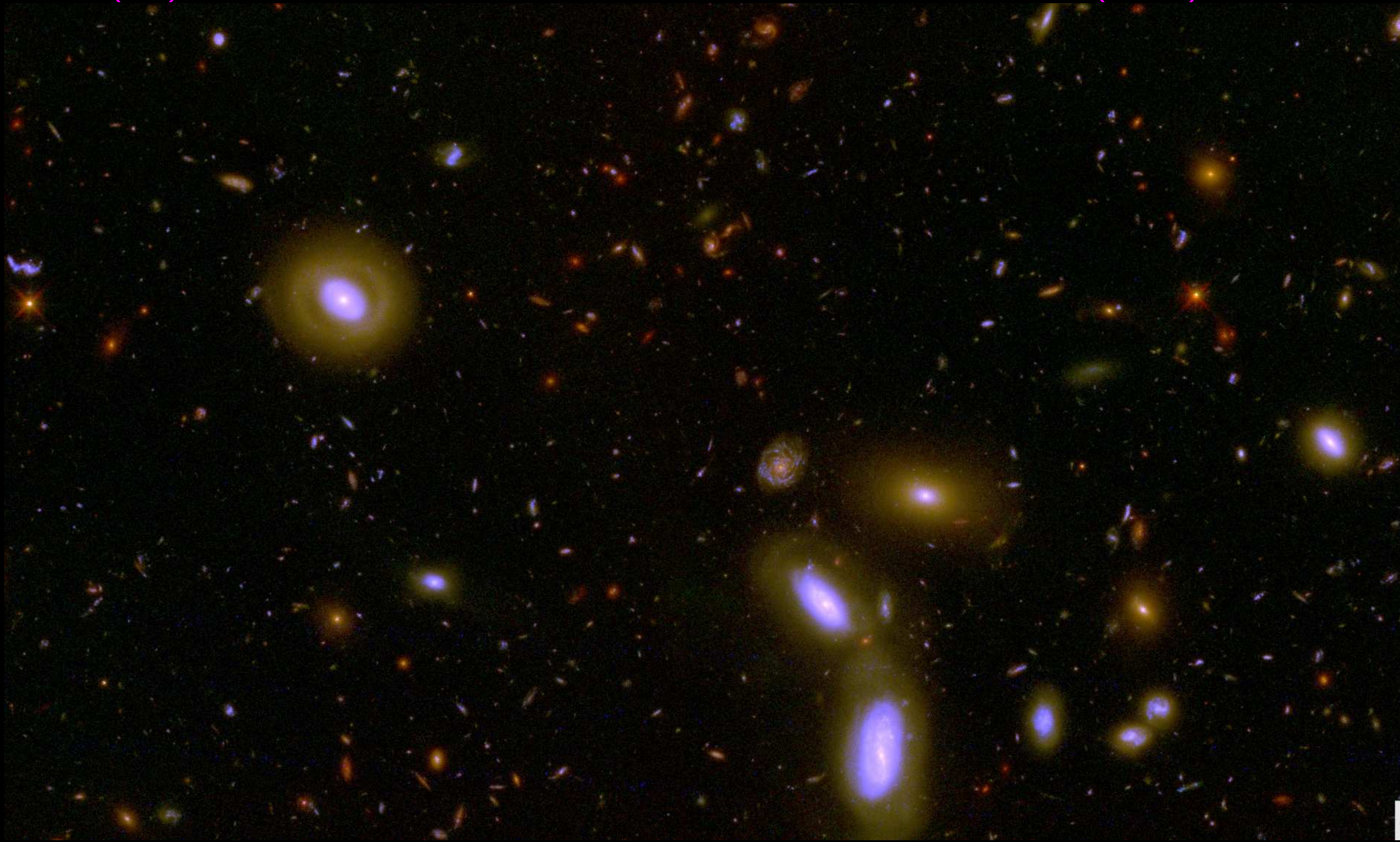

10 filters with HST/WFC3 & ACS reaching AB=26.5-27.0 mag (10-σ) over 40 arcmin^2 at 0.07–0.15" FWHM from 0.2–1.7μm (UVUBVizYJH).

(JWST adds 0.05–0.2" FWHM imaging to AB$\simeq$31.5 mag (1 nJy) at 1–5μm + 0.2–1.2" FWHM at 5–29μm, tracing young+old SEDs & dust).

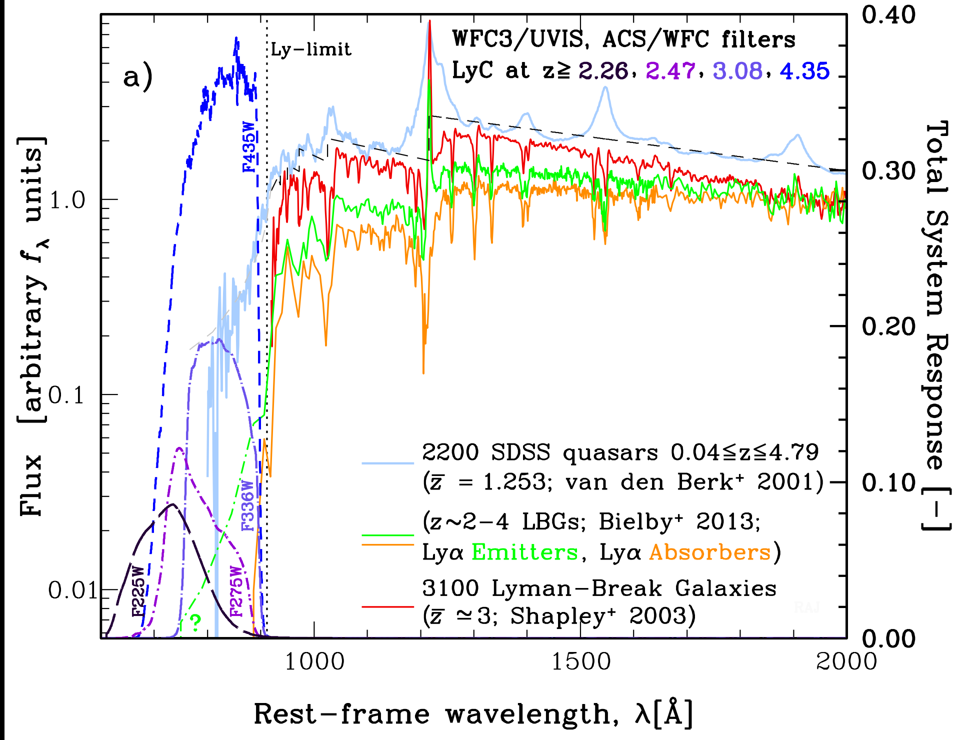

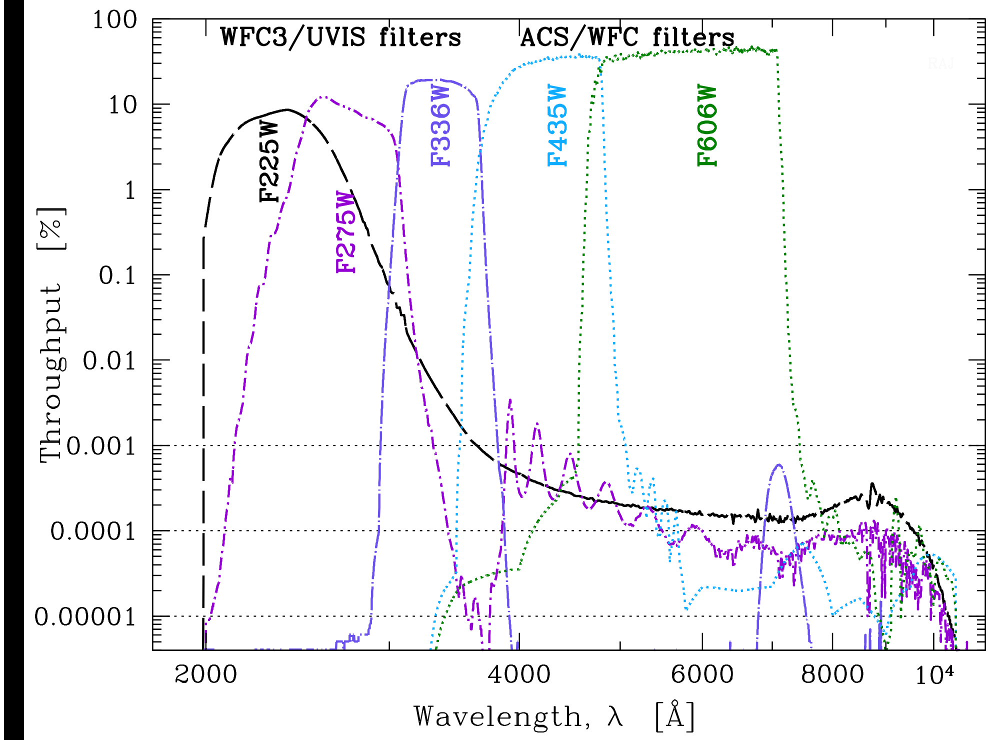

[LEFT] Composite rest-frame far-UV spectra of:

SDSS QSOs at z≃1.3 (van den Berk et al. 2001);

LBGs at z≃3 (Shapley et al. 2003);

LBGs at z≃2–4 (Bielby et al. 2013, Lyα emitters, & absorbers).

- WFC3/UVIS F225W, F275W, F336W, and ACS/WFC F435W filters can capture LyC (λ<912Å) at z$\geq$2.26, z$\geq$2.47, z$\geq$3.08, and z$\geq$4.35.
- Lower z-bounds: *no* $\lambda >$ 912Å below filter's red-edge ($\equiv$0.5% of peak).

[RIGHT] Total observed throughput curves, designed to maximize throughput and minimize red-leak, which is $\lesssim$0.6% of actual LyC signal.

- Filter red-leak wing ($\lambda \gtrsim$ 3648Å) is $\lesssim 3\times10^{-5}$ of peak transmission.

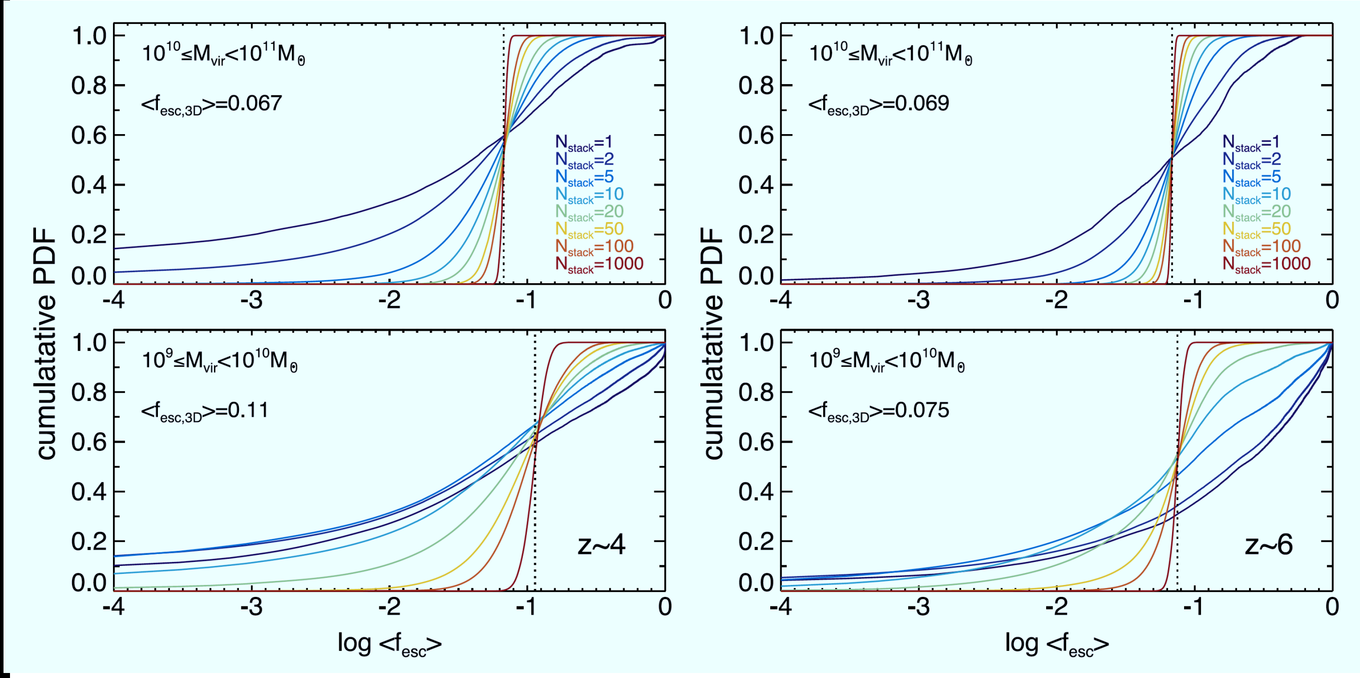

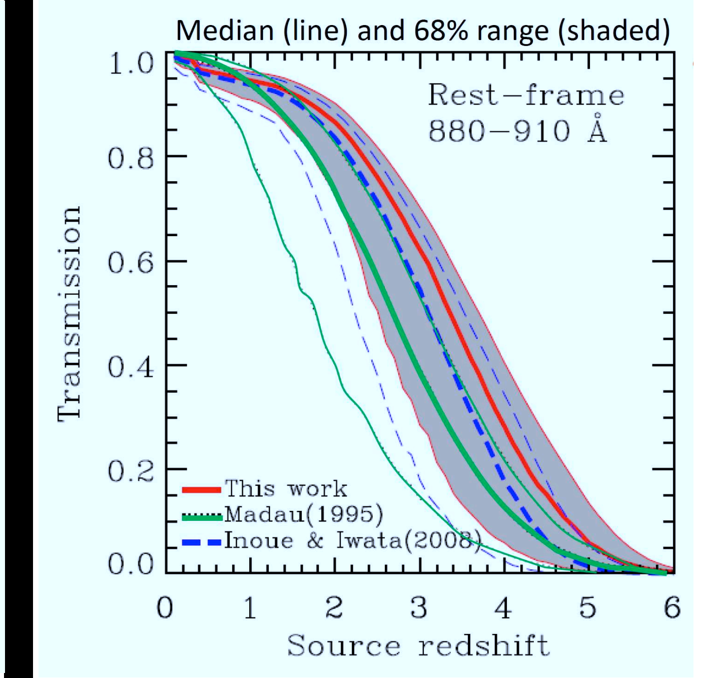

[LEFT] Cen & Kimm (2015): PDFs of mean f_{esc} over "N$_{stack}$" objects: high-mass (top) & low-mass (bottom) at z=4 (left) & z=6 (right).

- Mean f_{esc} from weighted number of photons mimics SED stacking of galaxy LyC data with true mean f_{esc} listed. ERS has N$_{stack}$=11–37.

[RIGHT] Inoue^{+} (2014): IGM transmission models for f_{esc}-calculations: Red is median and grey 68% range, based on MC simulations of $T_{IGM}(z)$.

- Uses updated absorber function+available data on Lyα forest, Damped Lyman Alpha (DLA) & Lyman Limit Systems (LLS) mean-free paths.
- We do stack z∼5 samples: (z∼5) AGN LyC ∼1^{m} brighter than galaxies.

(1b) Hubble WFC3 ERS — Spectroscopic Sample Selection

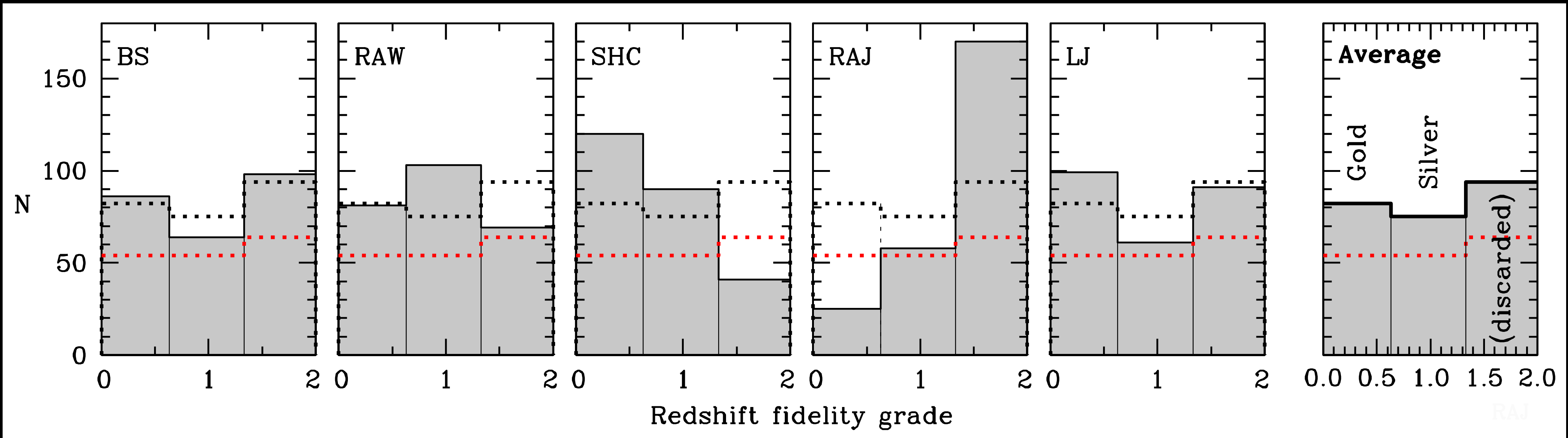

Comparison of redshift reliability (spectrum quality) assessments, from best (0.0) to poorest (2.0), by five co-authors [BS, RAW, SHC, RAJ, and LJ]:

- Measuring LyC escape fractions of $f_{esc} \simeq$6.0% at $\gtrsim 3\sigma$ requires low interloper fraction (Siana^{+} 2015; Vanzella^{+} 2015).
- Mask-out all interlopers from 10-band ERS mosaics to AB$\lesssim$27.5 mag.
- Use all VLT, Keck, & HST grism spectra to get most reliable samples:
- "Gold" sample: highest fidelity (grades=0–0.63): z_{sp}'s very likely correct.
- "Silver" sample: next highest fidelity (0.64–1.33), with z's likely correct.

(1b) Hubble WFC3 ERS — Spectroscopic Sample Selection

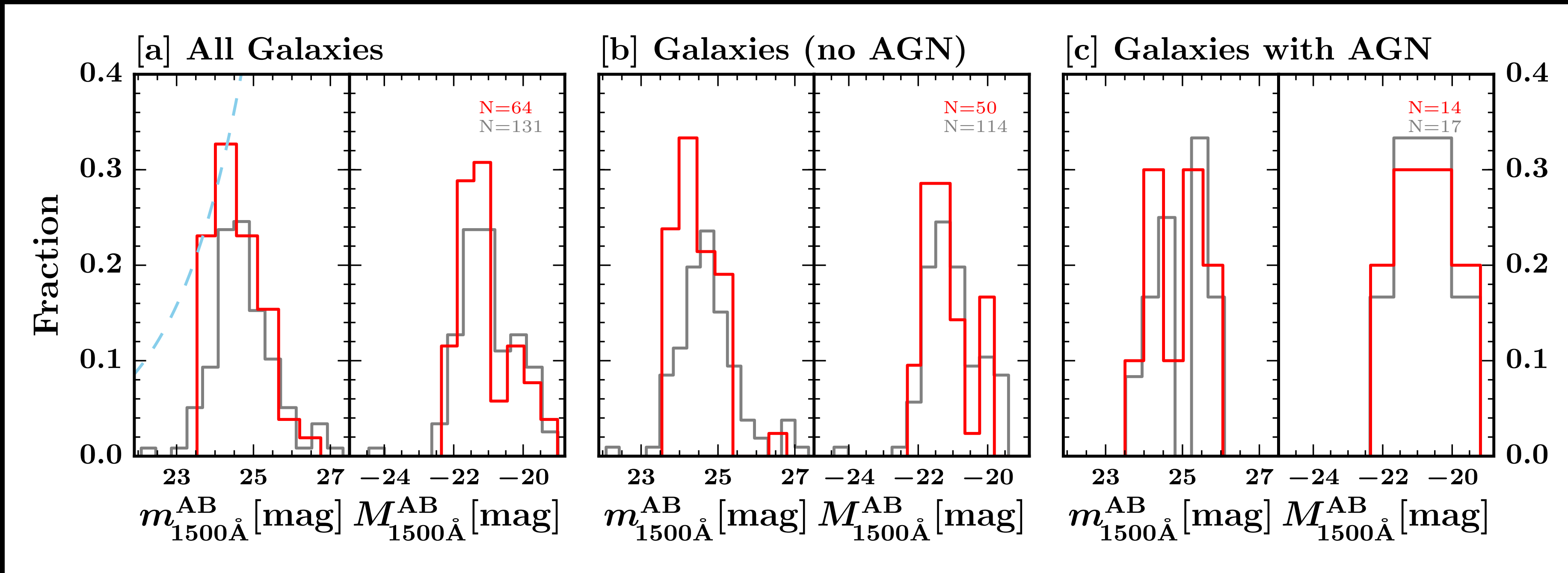

Apparent and absolute magnitude distributions (restframe 1550Å) of the "Gold" (highly reliable z) and "Gold+Silver" (reliable z's) samples:

- The blue dotted curve indicates the faint-end power-law slope of 0.16 dex/mag of the galaxy number counts of Windhorst+ (2011).
- Sample incompleteness for AB$\gtrsim$24, or M_{AB} (1650)$\gtrsim$–21 mag.
- LyC AB-fluxes & f_{esc} -values only valid for these selected luminosities.
- Galaxies with weak AGN have same N(M_{AB}) as galaxies without AGN.

(2) WFC3 & ACS Lyman Continuum Stacking, Systematics, & Fluxes

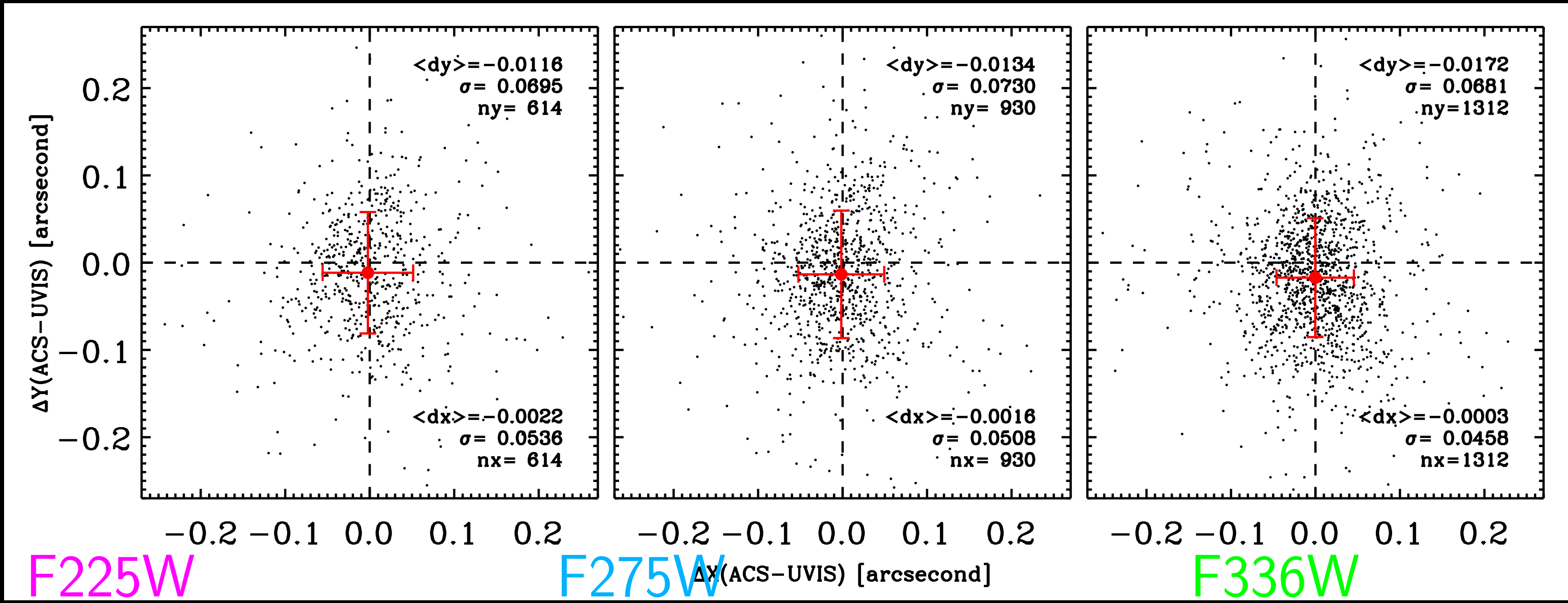

The first & hardest part was to get the WFC3 astrometry right:

- Pre-flight 2009 ERS geo-distortion had $\lesssim 0''.45$ offsets at image borders compared to GOODS v2.0 (Windhorst et al. 2011 ApJS, 193, 27).

- In-flight 2013 geo-distortion correction yielded excellent registration of all WFC3/UVIS tiles to the ACS F435W mosaics (Kozhurina et al. 2014).

- Compared to GOODS, all offsets are now $\lesssim 0''.02 \pm 0.06$ (rms) in all LyC filters (Smith et al. 2015) — this no longer blurs any LyC signal!

- Any LyC signal can now be measured and stacked, including removal of all foreground interlopers (AB$\lesssim$27.5), and measurement of LyC light-profiles.

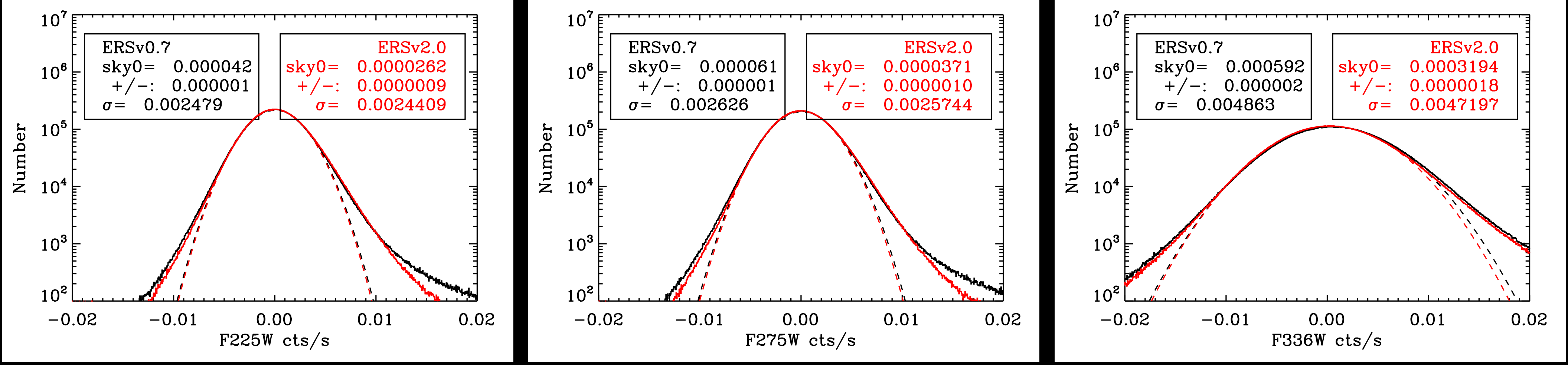

Residual sky-background levels in the drizzled WFC3/UVIS ERS mosaics:

- Black lines: Best fit to the 2009 ERS v0.7 mosaics of Windhorst et al. (2011), which used pre-flight thermal vacuum flat-fields.
- Red lines: Current mosaics (ERS v2.0; Smith et al. 2015), using best available on-orbit calibrations.
- Global *residual sky-background levels (in ADU/sec)* remaining after drizzling the ERS mosaics are ∼30.29, 29.99, and 28.15 mag arcsec^{-2} .
- Removed in 3 stages: globally during drizzling (zodi≃25.5 mag/″^{2}), locally before stacking, and again locally after stacking (to do photometry). This is absolutely critical for optimal LyC stacking.
- Final 71×71 pix (6.″39×6.″39) LyC stacks allow *residual* local sky-subtraction to ≲32.3 mag arcsec^{-2} .

(2) WFC3 & ACS Lyman Continuum Stacking, Systematics, & Fluxes

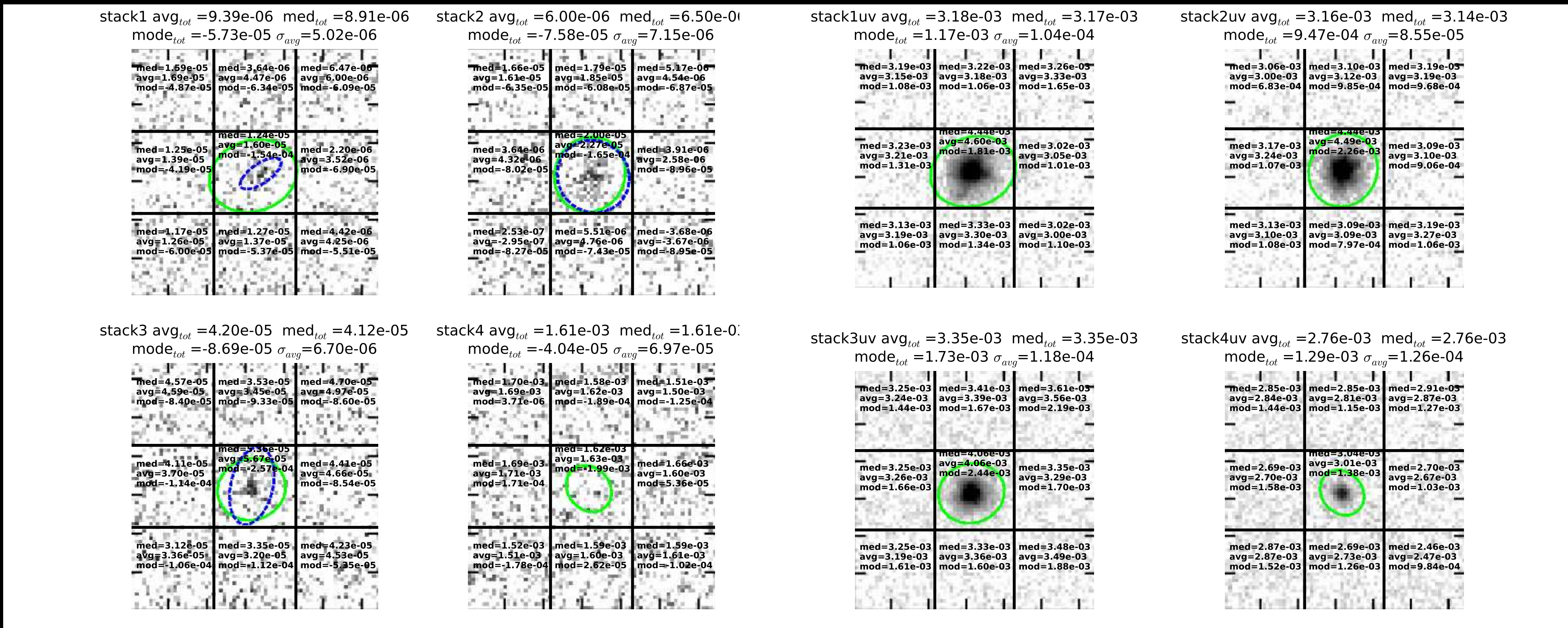

"Tic-tac-toe" sky-background analysis of 71×71 pixel (6.″39×6.″39) stacks: LyC [*left 4 panels*] and UVC [*right 4 panels*].

- Sky-background subtracted in 3 stages: *more globally* upon drizzling, *locally* before stacking, and *locally* before final photometry.

- Residual UV sky-gradients fainter than ∼32.3 mag arcsec^{-2} across photometric apertures.

- This is fainter than the LyC SB-signal where this can be measured, and may impose a (fundamental?) limit to how many images can be stacked.

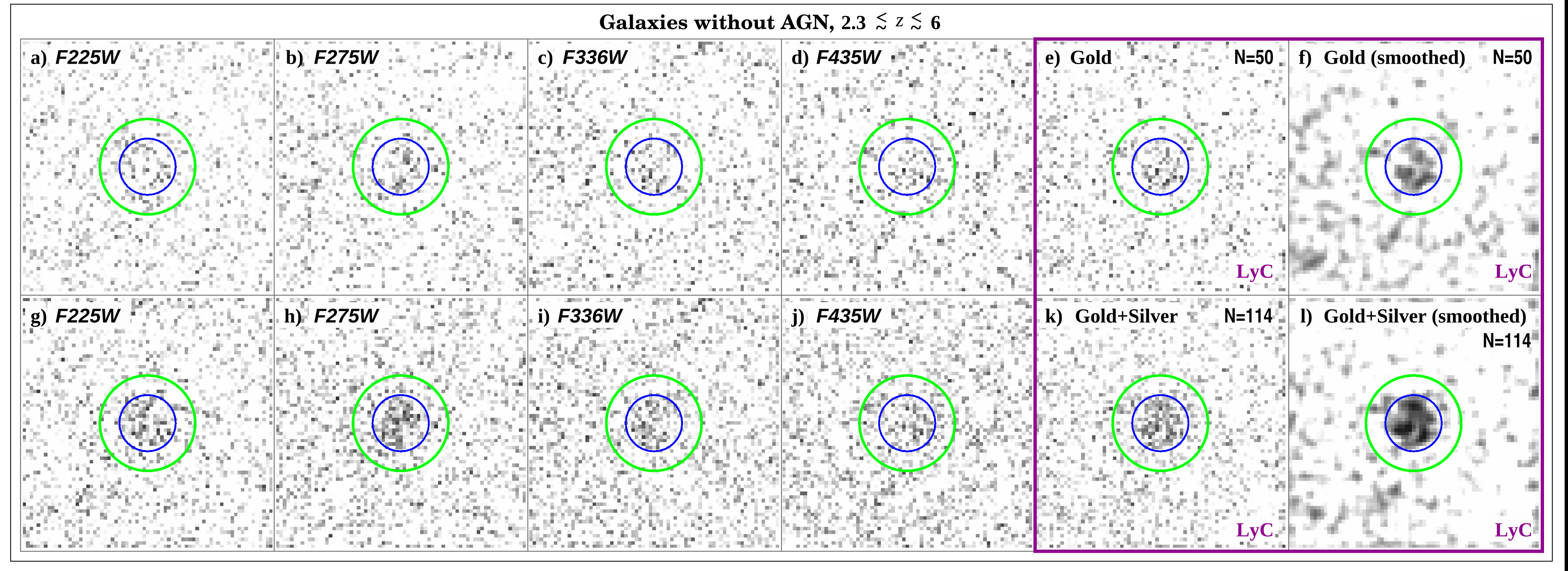

z=2.26–2.47 z=2.47–3.08 z=3.08–4.35 z=4.35–5.5 WEIGHTED ALL: z=2.26–5.5.

[*Top Row*]: All galaxies in combined Gold Galaxy sample: N=50;

[*Bottom Row*]: All galaxies in combined Gold+Silver sample: N=114.

[Right 2×2 panels]: Weighted "stack-of-stacks" over all 4 LyC filters: best visualizes LyC of galaxies at z≃2.3–5.5. Formal detection S/N-ratios:

$\gtrsim 7\sigma$ ($\sim\sqrt{50}\times 1.0\sigma$ above sky), $\gtrsim 13\sigma$ ($\sim\sqrt{114}\times 1.2\sigma$ above sky).

- Equivalent to 22–228 orbit UV stacks with HST, respectively.

Circles: r=8 ($0''\!.72$), 13 pix ($1''\!.17$), centered on the UVC emission.

(3) Stacked LyC Light-Profiles, & Weighted "Stack-of-Stacks"

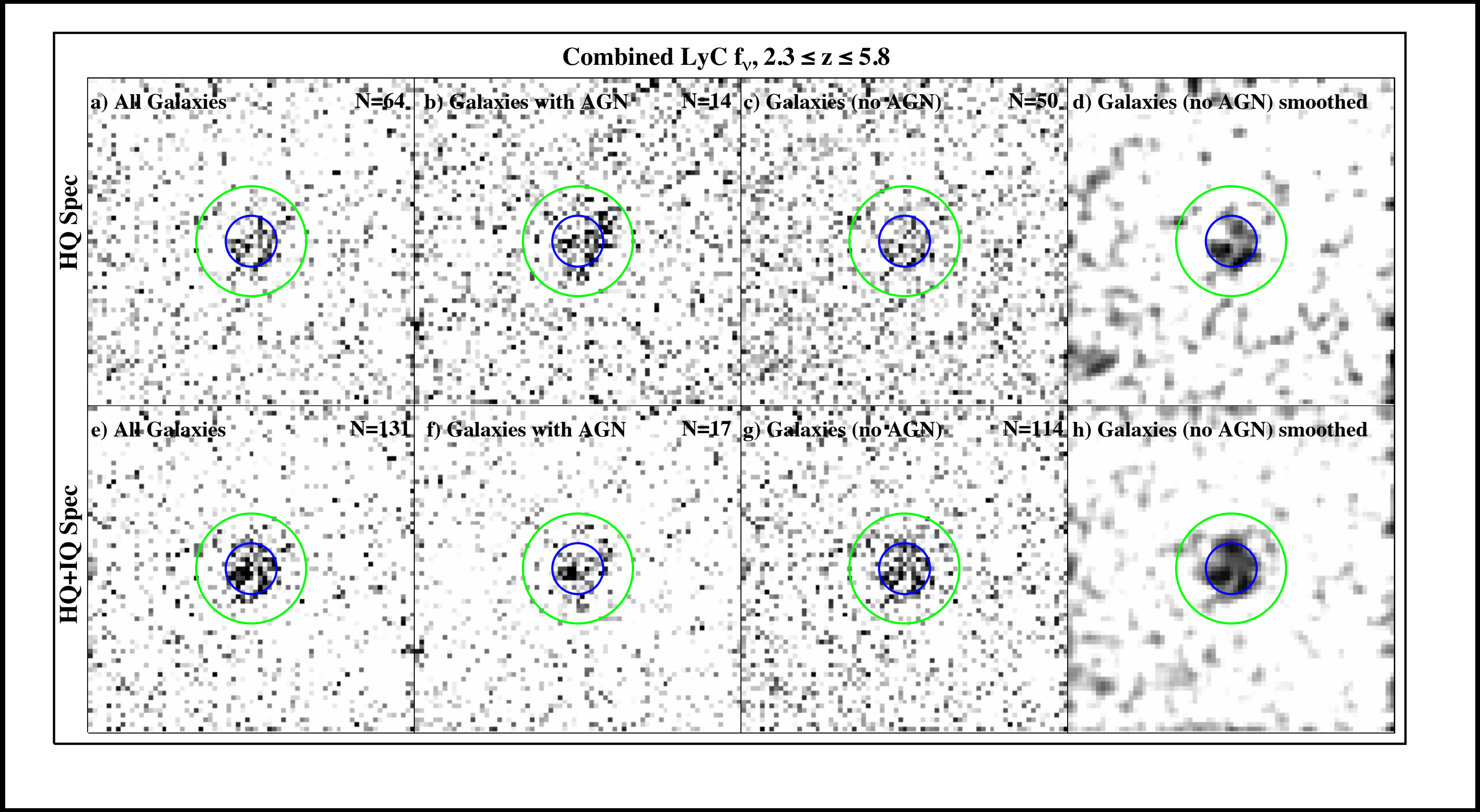

All Objects | Weak AGN | Galaxies w/o AGN | Smoothed Galaxies

[*Top Row*]: All Gold sample (z=2.3–5): 50 Galaxies + 14 weak AGN;

[*Bottom Row*]: All Gold+Silver sample (z=2.3–5): 114 Gxys + 17 AGN.

The faint LyC emission has a very flat SB-distribution with radius:

- Not centrally concentrated, with few clear sight-lines per galaxy.
- *On average* escapes along few random sight-lines through a porous ISM?
- Likeliest escape paths may be somewhat offset from galaxy center.

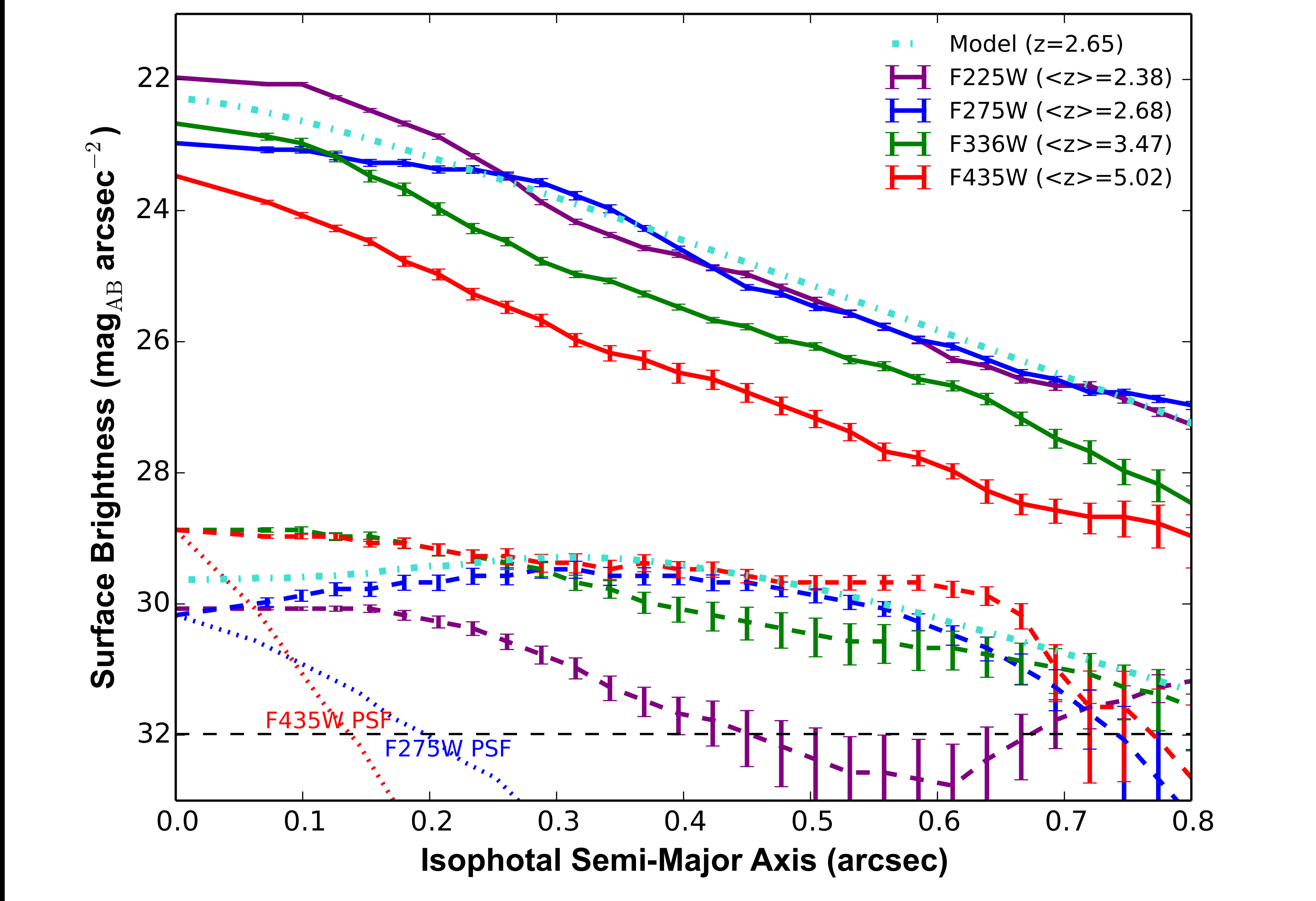

[*Top Curves*]: radial SB-profiles of stacked non-ionizing UVC (*solid*).

[*Bottom Curves*]: Radial SB-profiles of stacked LyC signal (*dashed*):

- All LyC SB-profiles are extended compared to the PSFs (dotted).
- Horizontal black dashed line is the 1σ SB-limit of $\sim$32 mag arcsec^{-2} .

Light-blue dot-dash: Dijkstra's z=2.68 UVC-scattering model with ISM porosity + escaping LyC increasing as: $f_{\rm cov}(r)=\mathcal{N}\,\exp\{-(r/10\,{\rm kpc})^x\}$.

(4) Spectral Energy Distribution (SED)-fitting & Dust (A_V)-distribution

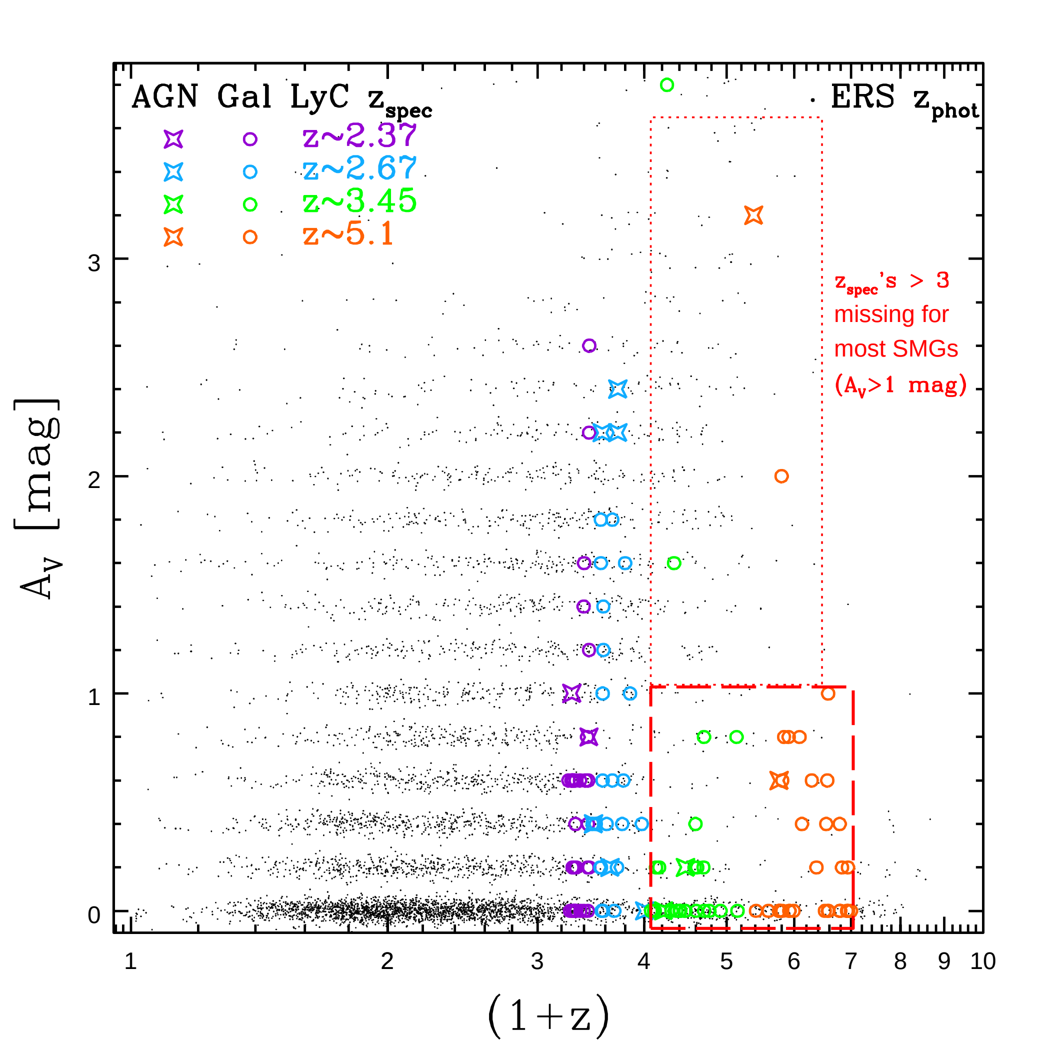

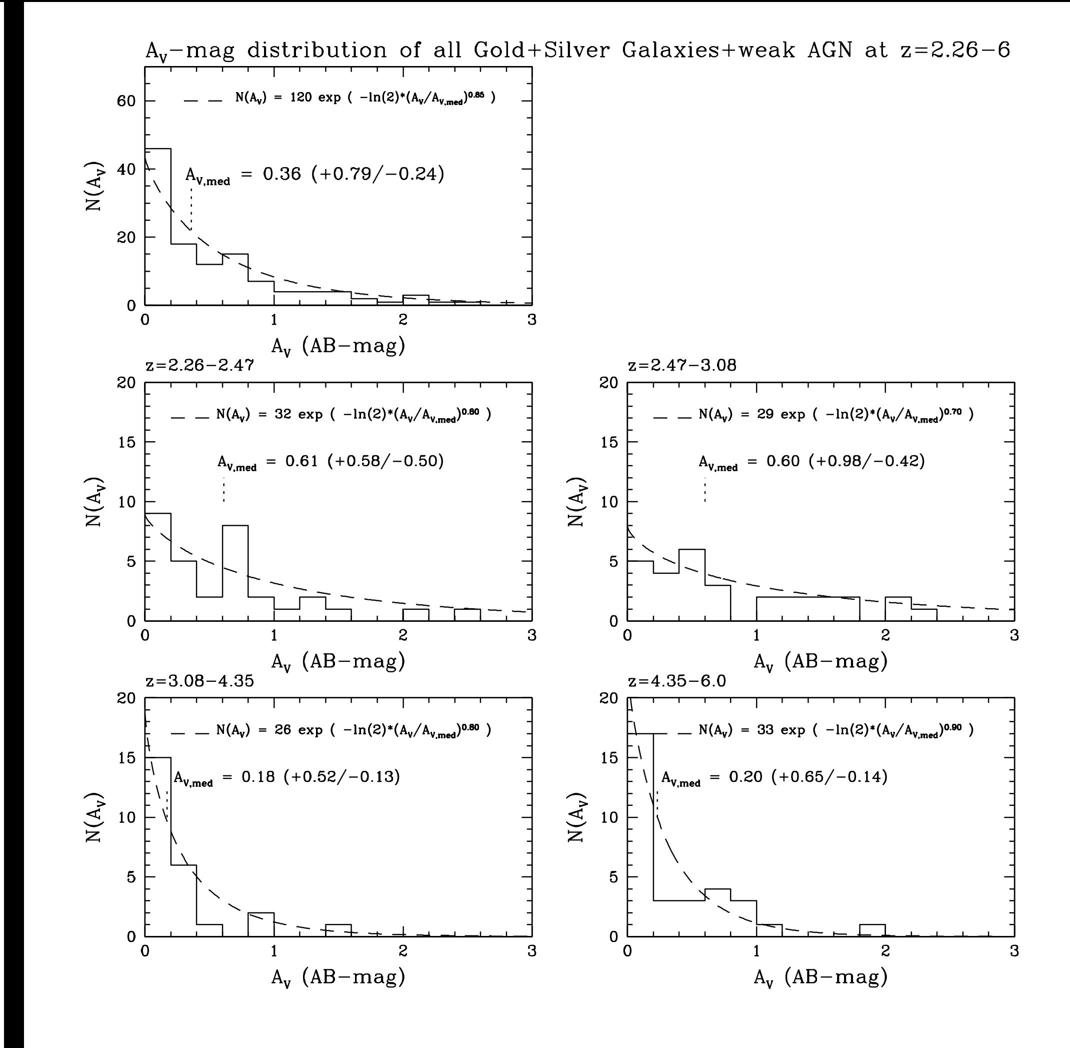

[LEFT]: Best-fit A_V from 10-band SEDs for all ERS galaxies (black dots).

Circles: galaxies; Asterisks: AGN at: z=2.37, z=2.68, z=3.45, z=5.1.

[RIGHT]: Adopted distributions N(A_V) for total Gold + Silver LyC samples:

Median A_V increases from $\sim 0.2^m$ at z=5.1–3.5 to $\sim 0.6^m$ at z=2.67–2.37.

Gxy+Agn selected at z_{sp}=3.45–5.1 miss ~45% of dusty ($A_V \gtrsim 1$) objects.

(5) LyC Escape Fractions vs. z for Faint Galaxies & Weak AGN

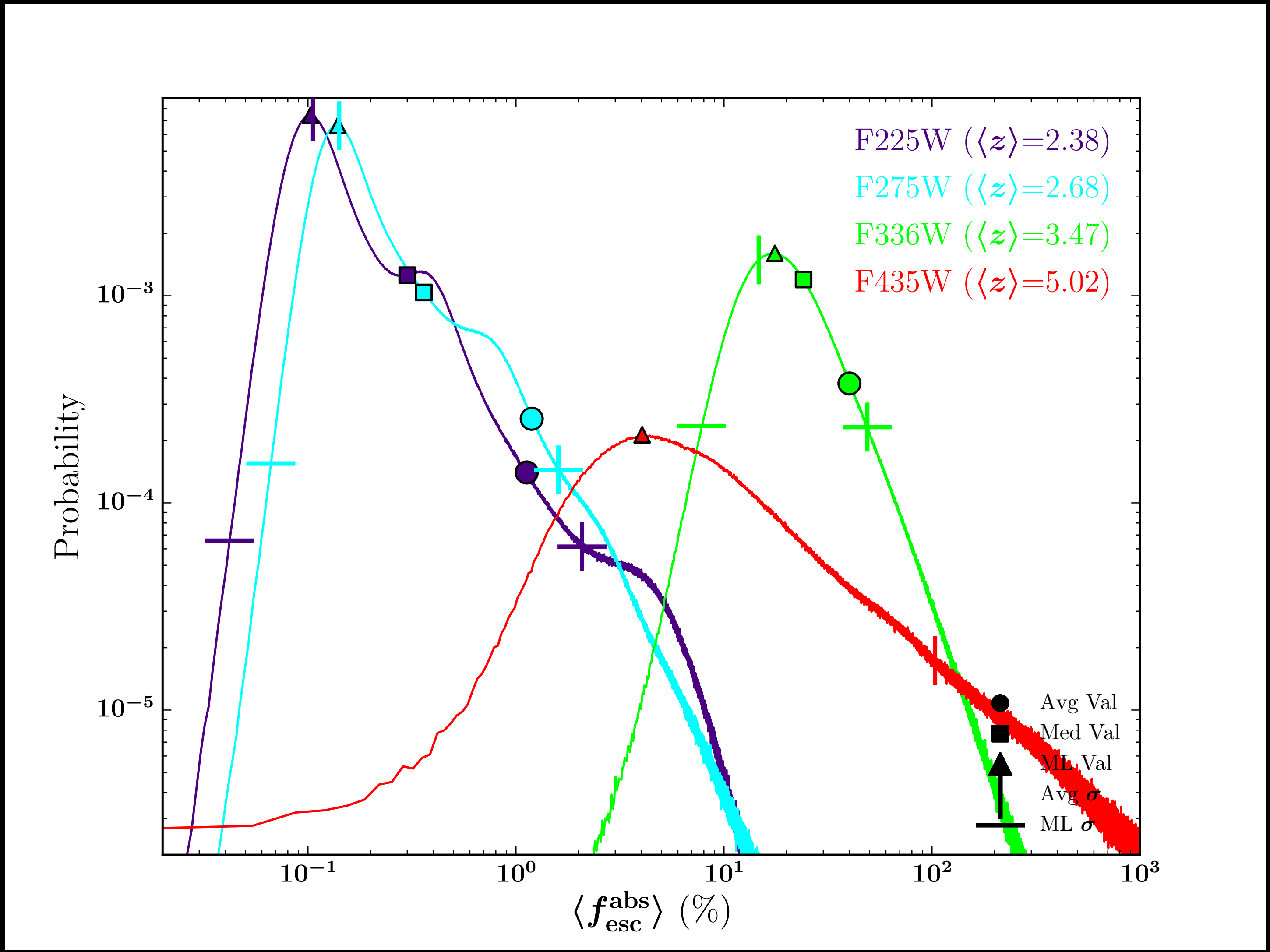

PDF of absolute f_{esc} -values (Inoue^{+} 2014 Monte Carlo), folding LyC fluxes $\pm$ 1σ errors through 10^9 random LOS of IGM transmission.

- Filled triangles indicate the resulting modal, and circles the average f_{esc} -values in each PDF. Tick-marks show the $\pm 1\sigma$ MC-range.

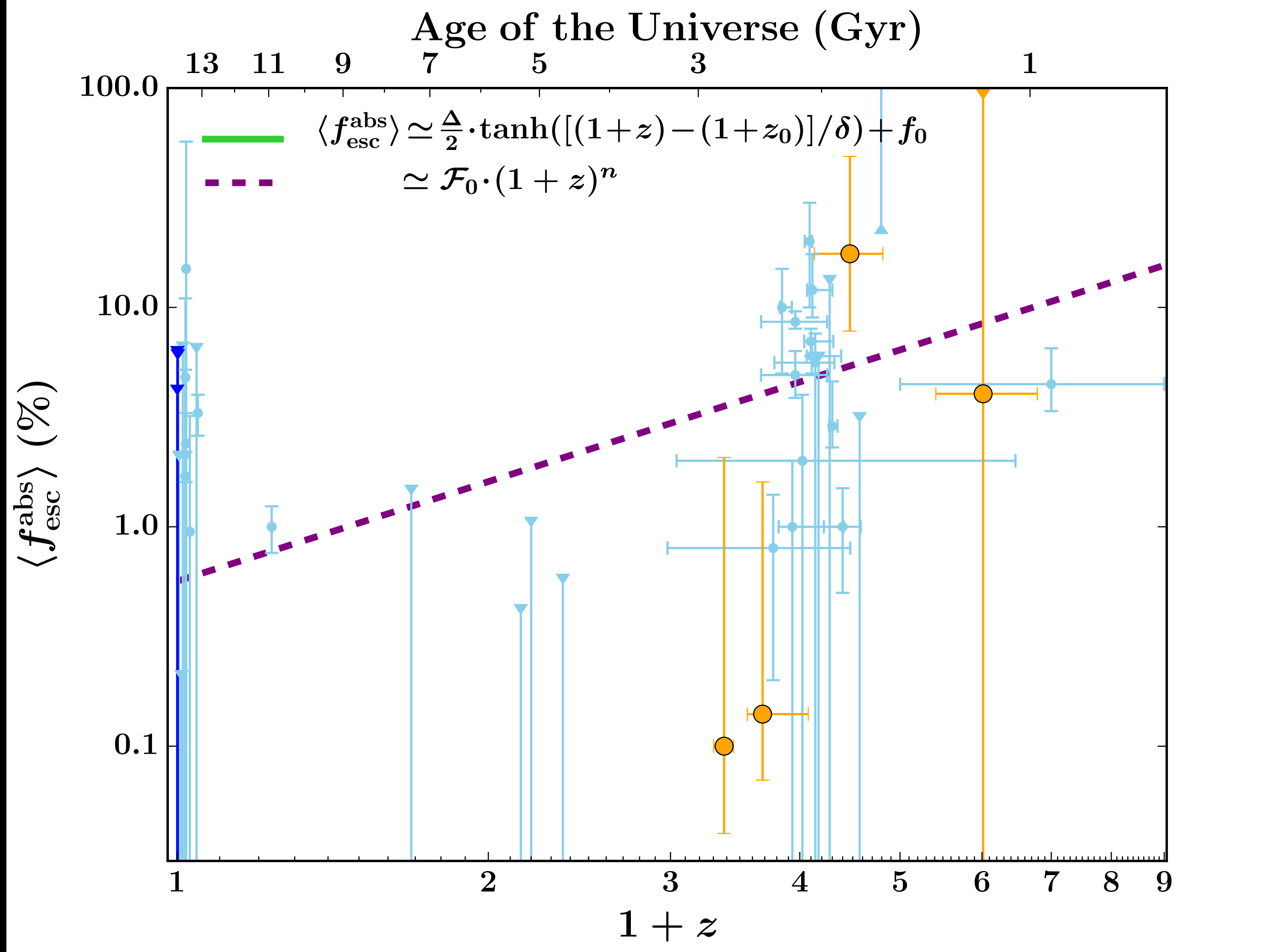

Absolute f_{esc} -z: Published + ERS Gold & Gold+Silver samples.

Single power law: $f_{esc}\simeq(0.006\pm0.002)\cdot(1+z)^{1.5\pm0.7}$ does not fit well.

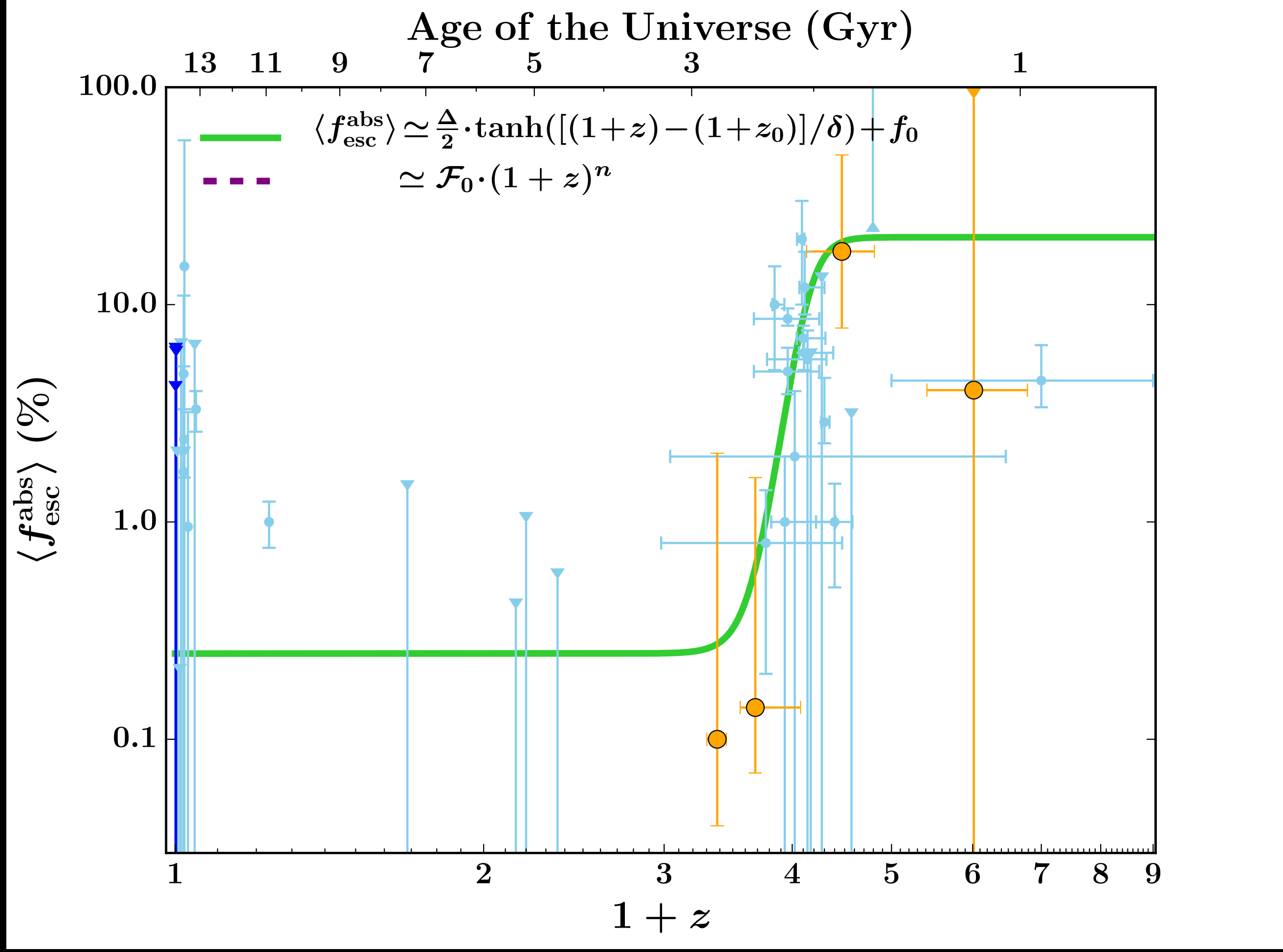

Absolute f_{esc} -z: Published + ERS Gold & Gold+Silver samples.

Single power law: $f_{esc} \simeq (0.006 \pm 0.002) \cdot (1+z)^{1.5 \pm 0.7}$ does not fit well.

Simple tanh[log(1+z)] captures more sudden f_{esc} -increase at z$\gtrsim$2.5–3.

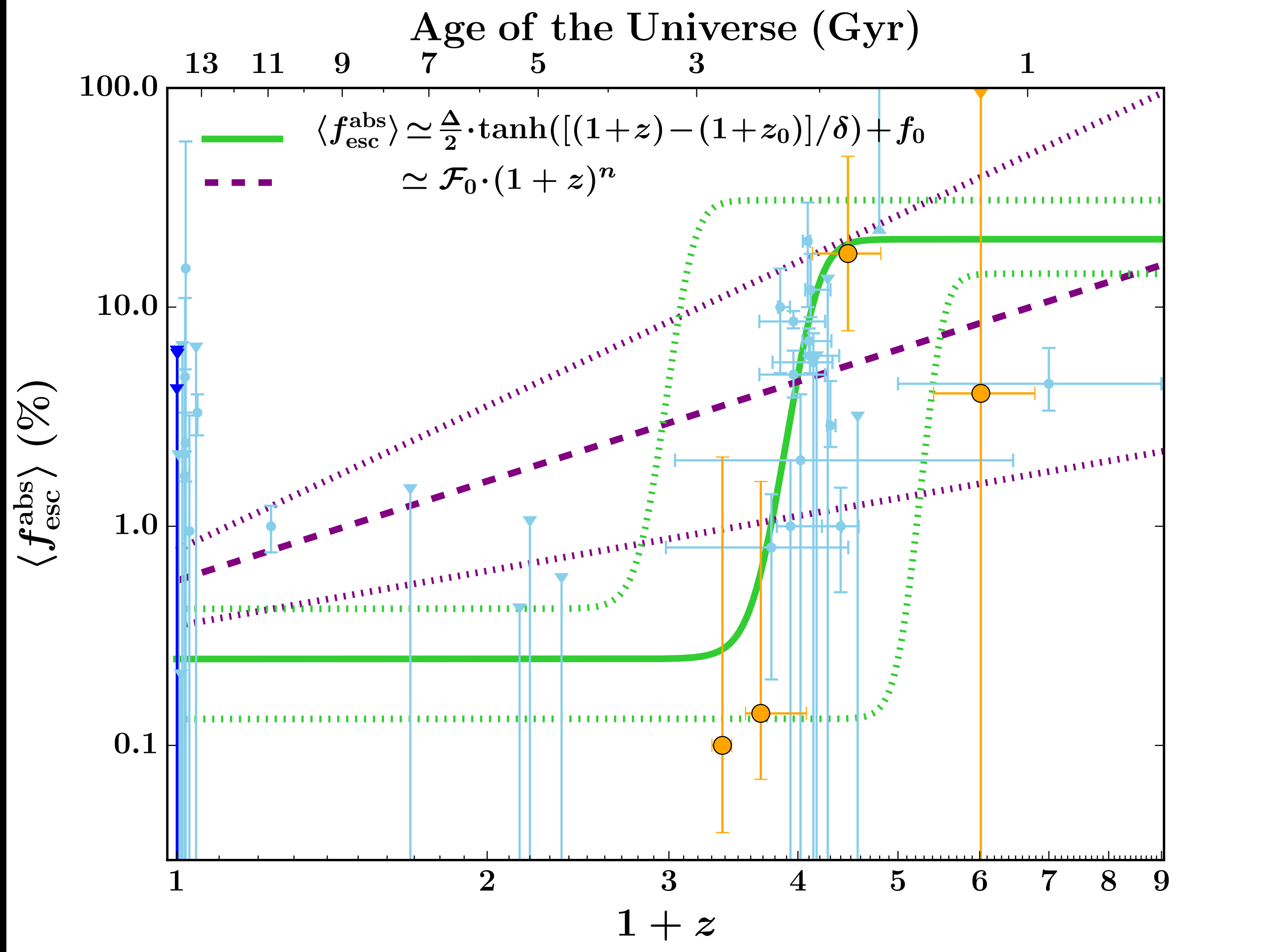

Absolute f_{esc} -z: Published + ERS Gold & Gold+Silver samples.

Power-laws: $f_{esc} \simeq (0.006 \pm 0.002) \cdot (1+z)^{1.5 \pm 0.7}$ do not fit well.

Simple tanh[log(1+z)] captures more sudden f_{esc} -increase at z$\gtrsim$2.5–3.

- f_{esc} of galaxies just high enough to cause reionization at z$\gtrsim$3.
- LyC of 17 weak AGN in ERS ∼1.0 mag brighter than for galaxies.
- Weak AGN may dominate and maintain reionization at z$\lesssim$3.

(6) What critical aspects will JWST add to HST's LyC Escape studies?

JWST FGS+NIRCam: R$\simeq$150, 0.8–5.0μm grism spectra to AB$\lesssim$28–29:

- Larger, fainter SED+z_{spec} -samples of LyC candidates in HST UV fields.

NIRSpec: JWST's short-wavelength ($\lambda\simeq$1–5.0μm) spectrograph:

- 100's of simultaneous faint-object spectra of LyC candidates to AB$\lesssim$27.5.

Concentrate on the most dusty (far-IR selected) $A_V\gtrsim$1 objects at z$\gtrsim$2.3!

Micro Shutters

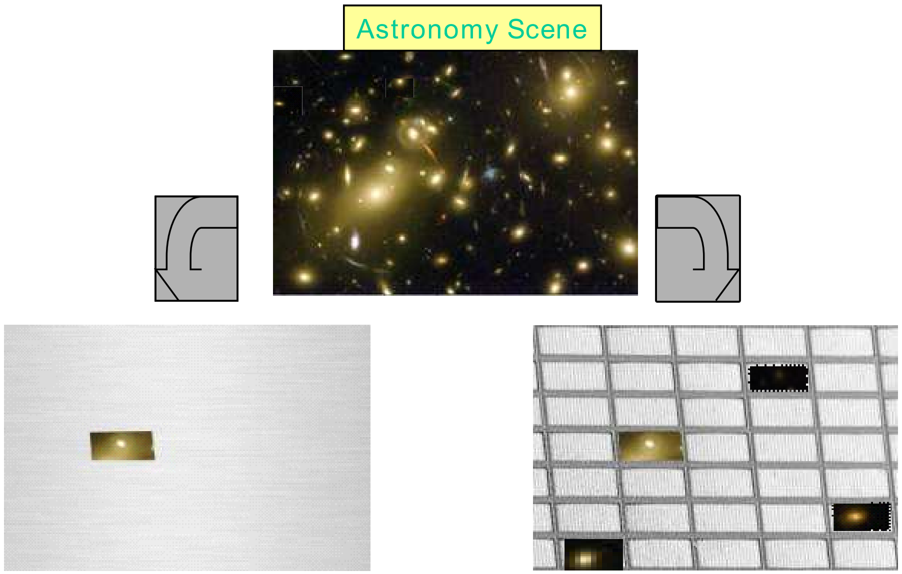

Metal Mask/Fixed Slit

Shutter Mask

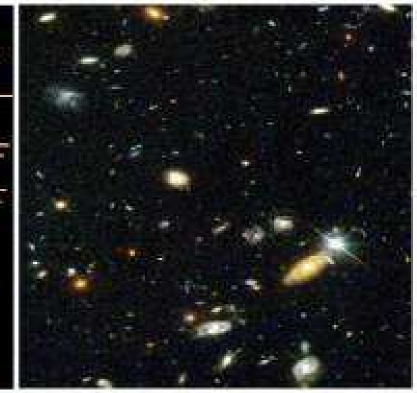

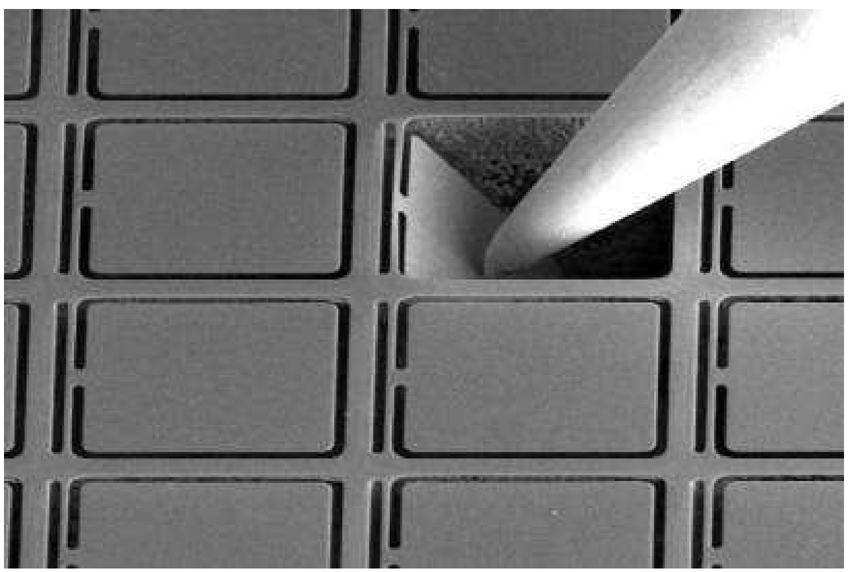

(7) Summary and Conclusions

(1) HST can measure LyC for galaxies + weak AGN at z$\simeq$2.26–5.

- WFC3 and ACS filters designed with low-enough redleak to enable this.
- Samples of sufficient size (N=11–114) need to be stacked to see LyC signal, preferably many dozen.
- Deepest 10-band images at HST resolution critical to mask-out all foreground interlopers to AB$\lesssim$27.5 mag.
- Careful spectroscopic redshift selection critical for reliable samples: Must correct for M_{AB} and A_V -biases.

(2) LyC signal detected in sub-samples of N=11–37 objects at z=2.26–5.

- Detections of AB(LyC) generally better than $\gtrsim$3–4σ (AB$\simeq$29.5–30.5 mag).
- Weak AGN have $\sim$1.0 mag brighter AB(LyC), but are 4–10$\times$ less numerous than galaxies.
- Stacked LyC SB-profiles are on average much flatter than the UV-continuum Sersic-profile.
- LyC may escape along few random sight-lines, offset from galaxy center: Non-Sersic, ISM-porosity increases with r?

(3) f_{esc} (z) may show rapid "tanh[log(1+z)]-like" increase at z$\gtrsim$2.5.

- Dust-corrected SED-fits and MC simulations essential to interpret this sudden drop in f_{esc} (z).
- Best-fit 10-band ERS SEDs suggests A_V increases from z$\sim$6 to z$\simeq$2.3.
- Spectroscopic selection at z=2.37–2.68 follows field galaxy A$_V$, but at z=3.45–5.1 misses $\sim$45% of dusty objects.
- Accumulating HI+A$_V$(t) may shut down f_{esc} (z$\lesssim$3), explaining a sudden f_{esc} -decrease at z$\gtrsim$3:

- f_{esc} (galaxies) just high enough to cause reionization at z$\gtrsim$3.
- (Galaxies with) weak AGN may dominate & maintain reionization at z$\lesssim$3.
- JWST NIRISS + NIRSpec spectra for (dusty) LyC objects to AB$\lesssim$28–29.

SPARE CHARTS

References and other sources of material shown:

http://www.jwst.nasa.gov/ & http://www.stsci.edu/jwst/

http://ircamera.as.arizona.edu/nircam/

http://ircamera.as.arizona.edu/MIRI/

http://www.stsci.edu/jwst/instruments/nirspec/

http://www.stsci.edu/jwst/instruments/fgs

Bielby, R., et al. 2013, MNRAS 430, 425

Bridge, C., et al. 2010, ApJ 720, 465

Bouwens, R. et al. 2015, ApJ, 803, 35

Gardner, J. P., et al. 2006, Space Science Reviews, 123, 485–606

Hathi, N. P., et al. 2010, ApJ, 720, 1708

Hathi, N. P., et al. 2013, ApJ, 765, 88

Inoue, A. K., Shimizu, I., Iwata, I., & Tanaka, M. 2014, MNRAS 442, 1805

Shapley, A., et al. 2003, ApJ 588, 65

Siana, B., et al. 2015, ApJ, 804, 15

Smith, B., Windhorst, R. A., Jansen, R. A., Cohen, S. H., Jiang, L., Dijkstra, M., Koekemoer, A. M., Bielby, R., Inoue, A. K., MacKenty, J. W., O'Connell, R. W., & Silk, J. I. 2015, AJ, in prep. Telescope Wide Field Camera 3 Observations of Escaping Lyman Continuum Radiation in Galaxies and Weak AGN at Redshifts $z \simeq 2.3$–5."

Vanden Berk, D. E., et al. 2001, AJ 122, 549

Vanzella, E., et al. 2015, A&A, 576, A116

Windhorst, R., et al. 2008, Advances in Space Research, 41, 1965

Windhorst, R., Cohen, S. H., Hathi, N. P., et al. 2011, ApJS, 193, 27

Yan, H., et al.2010, Res. in Astr. & Astrop., 10, 867

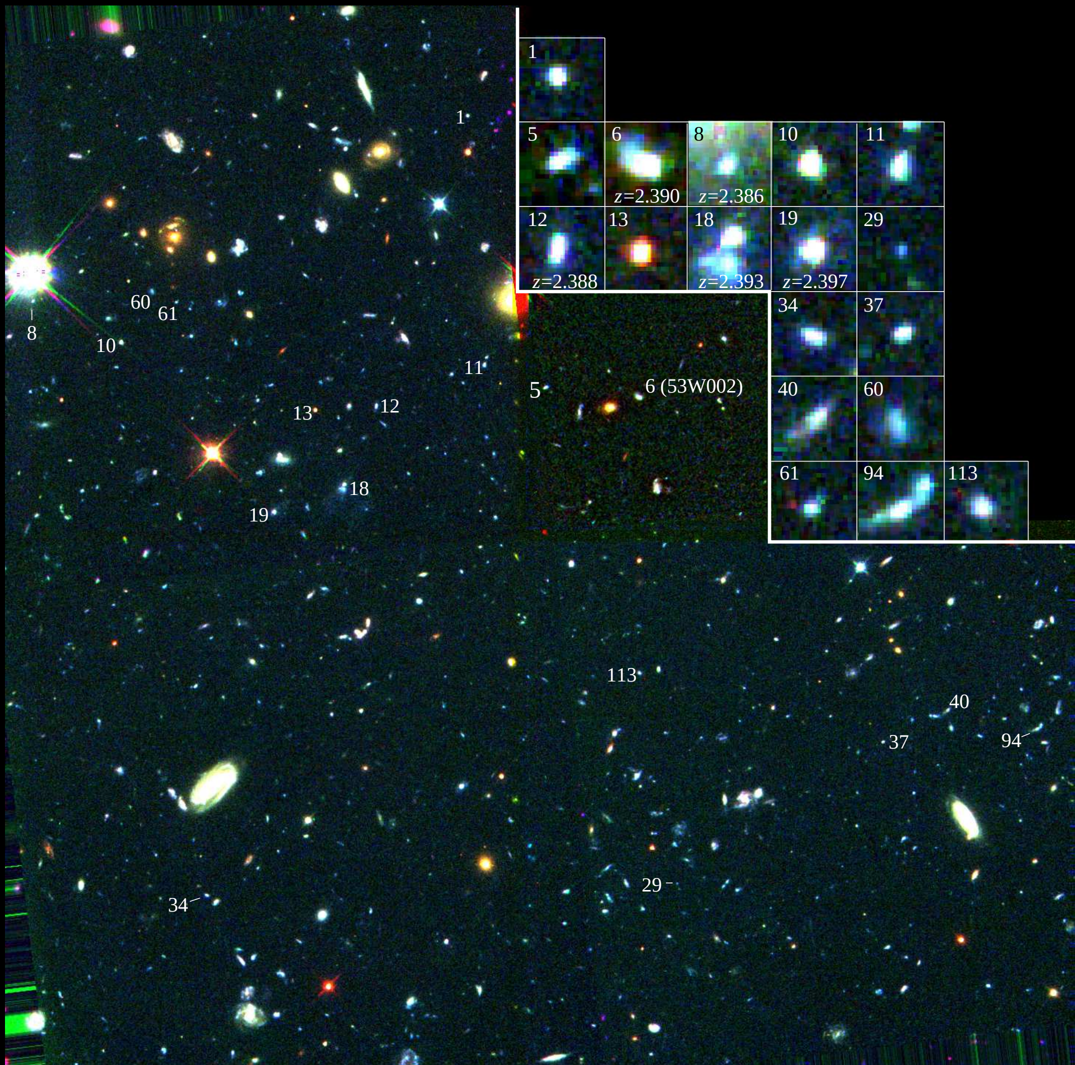

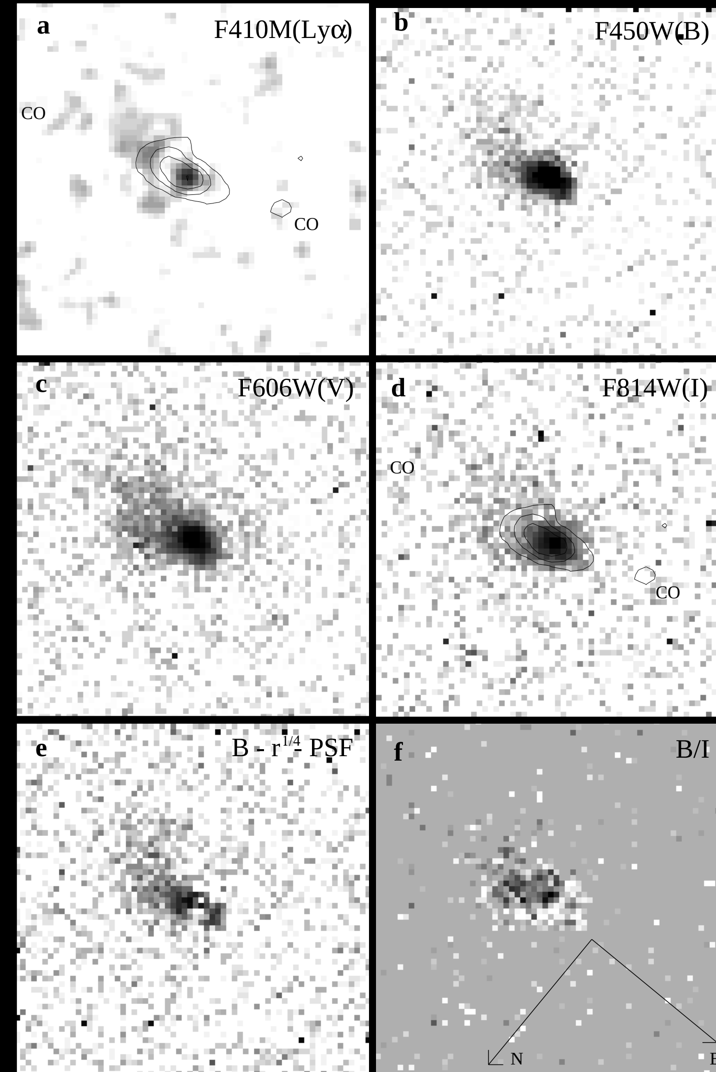

(Left): WFPC2 BVI + F410M (Lyα) on 53W002 + surrounding group of 17 z=2.39 Lyα candidates (Pascarelle et al. 1996, Nature, 383, 45).

(Right): HST/PC of radio galaxy 53W002 at z=2.390 (Windhorst et al. 1998, ApJL): stellar r$^{1/4}$-law + Lyα & blue continuum AGN-cloud.

$\Rightarrow$ May need to measure escaping LyC *outside* (dusty) LBGs with outflows.

JWST can measure AGN hosts $\lesssim$6 mag fainter in restframe UV-opt to z$\lesssim$15.

Table 2
LyC Stack Summaries of Gold and Combined Gold + Silver Samples

				LyC apertures				UVC apertures				
Filter (1)	z-range (2)	$\langle z \rangle$ (3)	$N_{\rm obj}$ (4)	$m_{\rm LyC}$ (5)	ABerr (6)	$SNR_{\rm LyC}$ (7)	$D_{\rm LyC}$ (8)	$m_{\rm LyC}$ (9)	$SNR_{\rm LyC}$ (10)	$D_{\rm LyC}$ (11)	$m_{\rm UVC}$ (12)	$SNR_{\rm UVC}$ (13)
GOLD GALAXIES WITH AGN:												
F225W	2.291–2.291	2.291	1	30.12	0.46	2.34	0.213	30.00	1.10	1.424	27.90	7.85
F275W	2.470–3.008	2.697	7	28.92	0.12	8.77	1.372	29.56	6.97	0.665	25.00	156.9
F336W	3.217–3.474	3.349	3	29.69	0.30	3.58	0.690	29.53	4.74	0.492	24.45	118.2
F435W	4.760–4.823	4.792	2	28.58	0.24	4.48	0.571	>31.5	<2	0.357	24.66	79.0
GOLD GALAXIES WITHOUT AGN:												
F225W	2.302–2.450	2.380	14	29.98	0.19	5.64	1.059	30.00	4.80	1.451	24.43	237.5
F275W	2.559–3.076	2.682	11	30.09	0.19	5.71	0.656	29.80	4.90	1.583	24.51	192.2
F336W	3.132–3.917	3.472	11	30.66	0.24	4.48	0.259	30.21	3.75	0.895	24.88	101.9
F435W	4.414–5.786	5.015	15	30.37	0.33	3.28	0.354	30.61	2.32	0.467	26.12	70.3
ALL GOLD GALAXIES:												
F225W	2.291–2.450	2.374	15	29.92	0.17	6.53	0.958	30.01	4.93	1.407	24.50	240.8
F275W	2.470–3.076	2.688	18	29.61	0.10	10.40	0.782	29.31	10.32	1.427	24.68	226.2
F336W	3.132–3.917	3.446	14	30.13	0.24	4.56	0.943	29.82	6.01	0.923	24.75	131.0
F435W	4.414–5.786	4.989	17	29.51	0.22	4.87	0.874	30.70	2.25	0.468	25.79	95.3
GOLD + SILVER GALAXIES WITHOUT AGN:												
F225W	2.262–2.450	2.362	31	29.79	0.11	9.46	1.109	29.71	8.74	1.576	24.56	303.6
F275W	2.481–3.076	2.692	26	29.46	0.09	11.92	1.135	29.35	11.29	1.606	24.76	229.6
F336W	3.110–4.149	3.524	24	29.96	0.16	6.85	1.017	29.93	6.83	1.073	24.73	164.9
F435W	4.414–6.277	5.312	37	30.35	0.19	5.79	0.452	31.53	2.23	0.336	26.72	92.7
ALL GOLD + SILVER GALAXIES:												
F225W	2.262–2.450	2.362	33	29.88	0.12	9.27	1.017	29.72	8.63	1.620	24.59	295.7
F275W	2.470–3.076	2.669	33	29.34	0.07	15.11	1.082	29.22	14.03	1.627	24.79	252.7
F336W	3.110–4.149	3.505	27	30.01	0.16	6.94	1.036	29.93	7.19	1.089	24.68	188.2
F435W	4.379–6.277	5.263	40	29.84	0.15	7.33	0.669	30.08	5.83	0.668	26.22	103.1

Table 3
Summary of $f_{\rm esc}$ Constraints

$\langle z \rangle$	N_{obj}	$\langle f_{\rm LyC}/f_{1500}(Obs)\rangle$	$\langle f_{1500}/f_{LyC}(Int)\rangle$	$A_{V\,med}$	$\langle \mathcal{T}_{\rm IGM} \rangle$	$f^{\rm rel}_{\rm esc,600}$	$f^{\rm rel}_{\rm esc,700}$	$f^{\rm rel}_{\rm esc}$(IGM-MC)	$f^{\rm abs}_{\rm esc}$(IGM-MC)
(1)	(2)	(3)	(4)	(5)	(6)	(7)	(8)	(9)	
GOLD GALAXIES *with* AGN:									
2.291	1	0.129 ±0.0577	$3.44^{+0.13}_{-0.10}$	$0.90^{+0.14}_{-0.14}$	$0.297^{+0.081}_{-0.083}$	$\gtrsim$100%	$\gtrsim$100%	—	—
2.677	7	0.0270 ±0.00309	$2.98^{+0.08}_{-0.07}$	$1.23^{+1.14}_{-1.13}$	$0.247^{+0.085}_{-0.085}$	25^{+18}_{-16}%	33^{+24}_{-22}%	—	—
3.349	3	0.00802 ±0.00224	$11.4^{+0.20}_{-0.14}$	$0.10^{+0.14}_{-0.10}$	$0.112^{+0.049}_{-0.049}$	79^{+48}_{-48}%	82^{+50}_{-50}%	—	—
4.792	2	0.0158 ±0.00389	$3.55^{+0.37}_{-0.26}$	$1.90^{+0.50}_{-0.50}$	$0.00108^{+0.00122}_{-0.00107}$	∼100%	∼100%	—	—
GOLD GALAXIES WITHOUT AGN:									
2.380	14	0.00213 ±0.000568	$3.44^{+0.13}_{-0.10}$	$0.55^{+0.70}_{-0.44}$	$0.297^{+0.081}_{-0.083}$	$3.7^{+2.8}_{-2.8}$%	$7.0^{+5.3}_{-5.3}$%	$0.76^{+15}_{-0.35}$	$0.11^{+2.16}_{-0.05}$
2.682	11	0.00586 ±0.00103	$2.98^{+0.08}_{-0.07}$	$0.58^{+0.89}_{-0.40}$	$0.247^{+0.085}_{-0.085}$	$5.3^{+4.5}_{-4.5}$%	$7.1^{+6.0}_{-6.0}$%	$3.22^{+35}_{-1.08}$	$0.27^{+2.96}_{-0.09}$
3.472	11	0.00488 ±0.00109	$11.4^{+0.20}_{-0.14}$	$0.18^{+0.64}_{-0.12}$	$0.112^{+0.049}_{-0.049}$	48^{+29}_{-29}%	50^{+31}_{-31}%	34^{+63}_{-16}	32^{+57}_{-15}
5.015	15	0.0200 ±0.00609	$3.55^{+0.37}_{-0.26}$	$0.17^{+0.67}_{-0.12}$	$0.00108^{+0.00122}_{-0.00107}$	∼100%	∼100%	∼100%	$\gtrsim 21^{+79}_{-2}$
GOLD + SILVER GALAXIES WITHOUT AGN:									
2.362	31	0.00809 ±0.000857	$3.74^{+0.12}_{-0.10}$	$0.55^{+0.70}_{-0.44}$	$0.306^{+0.055}_{-0.055}$	$5.2^{+3.7}_{-3.7}$%	$9.9^{+7.0}_{-7.0}$%	$1.76^{+15}_{-0.67}$	$0.26^{+2.22}_{-0.10}$
2.692	26	0.0132 ±0.00111	$3.25^{+0.06}_{-0.06}$	$0.58^{+0.89}_{-0.40}$	$0.249^{+0.052}_{-0.054}$	$12.7^{+7.3}_{-8.2}$%	$17^{+9.7}_{-10.7}$%	$6.2^{+27}_{-2.1}$	$0.55^{+2.40}_{-0.18}$
3.524	24	0.00809 ±0.00118	$4.33^{+0.34}_{-0.30}$	$0.18^{+0.64}_{-0.12}$	$0.089^{+0.027}_{-0.027}$	37^{+17}_{-20}	39^{+18}_{-21}%	$6.5^{+25}_{-3.1}$	$24^{+68}_{-1.0}$
5.312	37	0.0353 ±0.00611	$2.97^{+0.13}_{-0.15}$	$0.17^{+0.67}_{-0.12}$	$0.00019^{+0.00152}_{-0.00154}$	∼100%	∼100%	87^{+113}_{-55}	$\gtrsim 20^{+80}_{-2}$

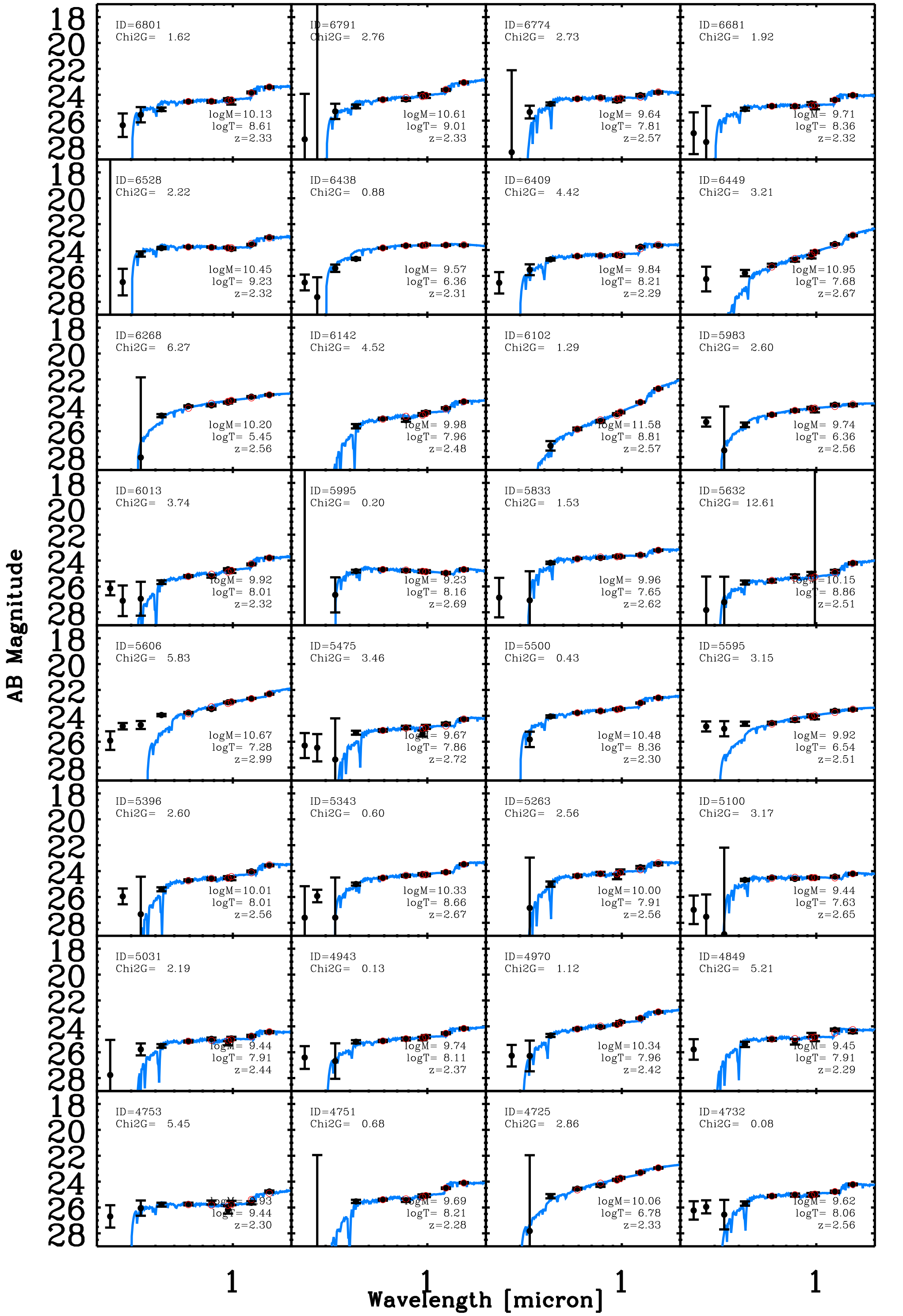

Example of SED fits used for f_{esc} (MC) etc, using $\lambda \gtrsim 1216$ Å and $z \equiv z_{spec}$.

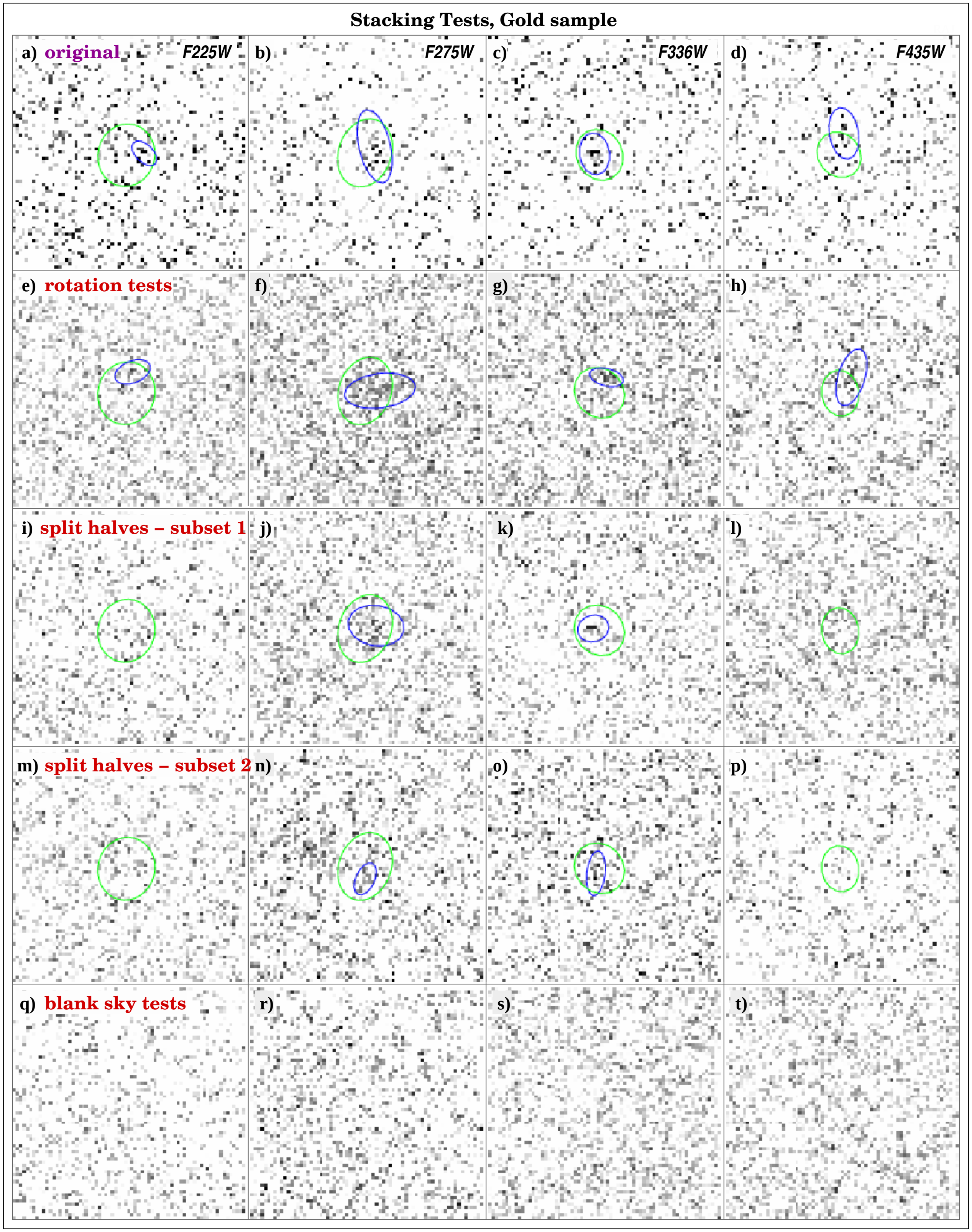

z=2.37, z=2.68, z=3.45, z=5.1 Gold stacks;

Same Gold stacks after random 90° rotation;

First independent data halves Gold stacks;

Second independent data halves Gold stacks;

Random sky-stacks to verify null-signal.

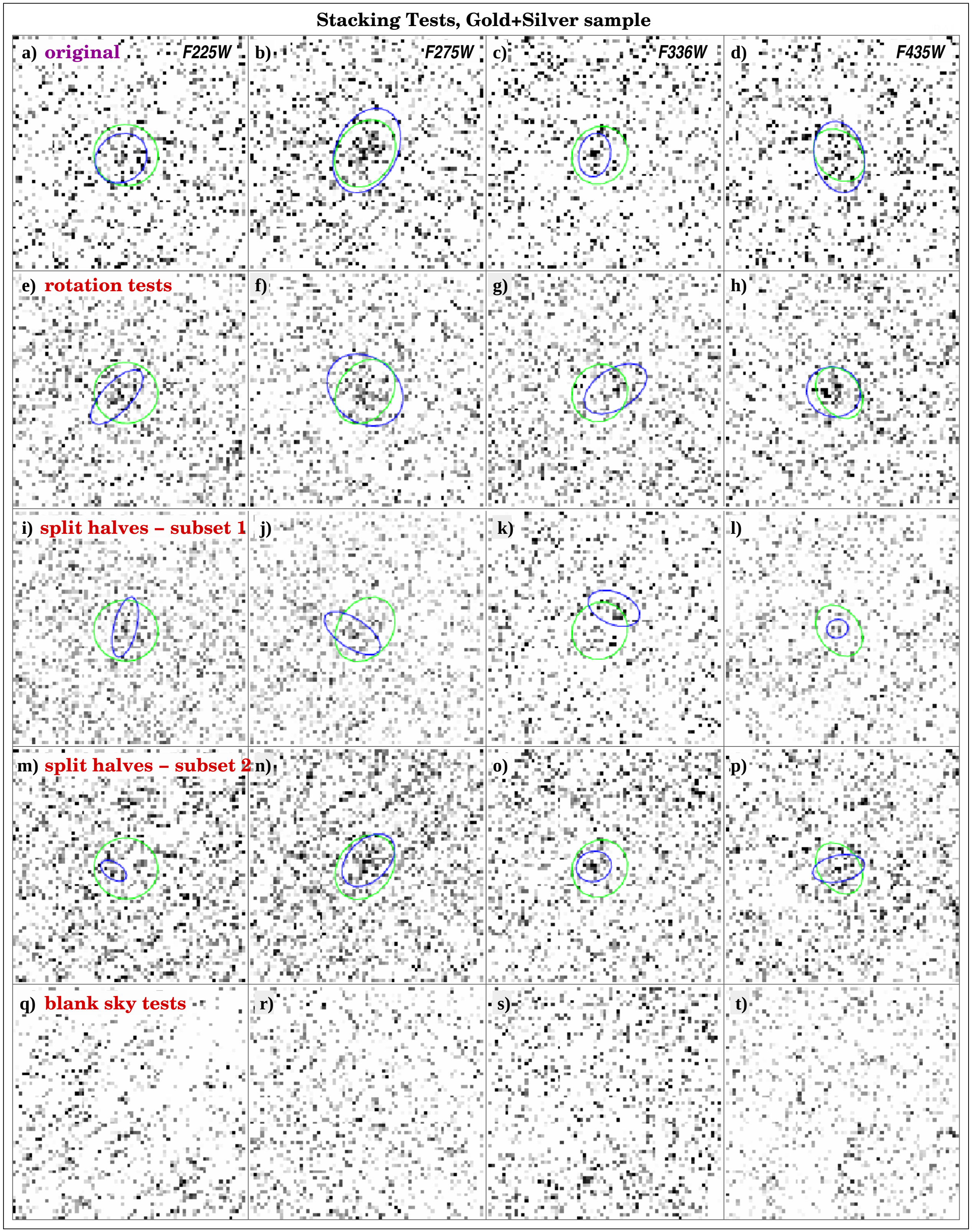

z=2.37, z=2.68, z=3.45, z=5.1 Silver stacks;

Same Silver stacks after random 90° rotation;

First independent data halves Silver stacks;

Second independent data halves Silver stacks;

Random sky-stacks to verify null-signal.

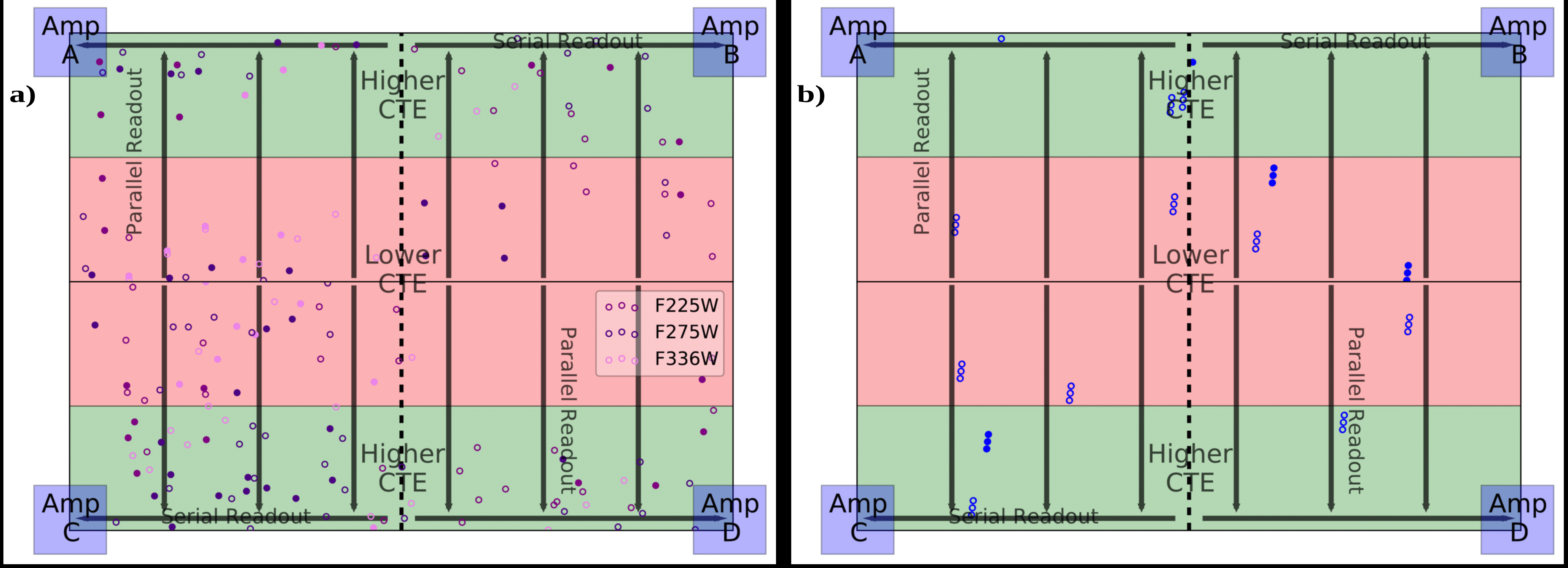

Detector location of "high-CTE" and "low-CTE" sub-samples: [LEFT]: WFC3/UVIS F225W, F275W, F336W. [RIGHT]: ACS/WFC F435W.

Green regions are closest to parallel read-out amplifier. Red regions are furthest from amplifiers, and may suffer more from CTE-degradation.

- Filled circles show marginal LyC signal in individual objects:
- These are fairly uniformly distributed across individual CCDs.

Average stacked LyC diff: Δ(Lower-CTE–High-CTE) $\simeq$ 0.5$\pm$0.35 mag.

$\Longrightarrow$ Less than four months after WFC3's launch, CTE-induced systematics are not yet larger than the random errors in the LyC signal.